REVIEW

Organometallic Materials for Nonlinear Optics

Hari Singh Nalwa

Hitachi Research Laboratory, Hitachi Ltd, 4026 Kuji-cho, Hitachi-shi, Ibaraki 319-12, Japan

Almost three decades ago, the field of nonlinear optics evolved with the discovery of lasers. In the beginning, nonlinear optical (NLO) phenomena were investigated in inorganic materials, leading to the development of traditional NLO materials such as lithium niobate, potassium titanyl phosphate, quartz and gallium arsenide. In the 1970s, the importance of organic materials was realized because of the promise of large NLO responses, high laser damage thresholds, fast optical responses, architectural flexibility and ease of fabrication. Following work with organic materials, the scrutiny of organometallics also began recently. In organometallics, the metal–ligand bonding is expected to display large molecular hyperpolarizability because of the transfer of electron density between the metal atom and the conjugated ligand system. In organometallics, the diversity of central metals, oxidation states and ligands fosters in optimization of the charge-transfer interactions. Keeping this in view, second- and third-order NLO properties of organometallics have been reviewed here, highlighting new materials that are emerging. Organometallics may have a wide range of applications in opto-electronics including integrated optics, optical switching, telecommunications, bistability and modulation.

Keywords: Nonlinear optics, second-order nonlinear optical effects, third-order nonlinear optical effects, organometallics, molecular hyperpolarizability, central metals, conjugated ligands, oxidation states, applications, opto-electronics

CONTENTS

1 INTRODUCTION

In 1960, Maiman[1] developed the first operating laser using a crystal of ruby. One year later, Franken et al.[2] demonstrated that when a beam of red light from a ruby laser is illuminated in a quartz crystal, the frequency of the emerging ultraviolet component was doubled compared with the incoming red light. This double-frequency phenomenon is termed the 'second harmonic'. With these landmark discoveries, two fields of research evolved concurrently: laser science on one hand, and work on nonlinear optics focused on second harmonic generation (SHG) on the other. Following the discovery of Franken et al., the concept of phase matching was shown in birefringent crystals[3-6] and many other

interesting nonlinear optical (NLO) phenomena were also discovered.[7-10] Simultaneously, theoretical programmes for the understanding of nonlinear optical interactions also began to pursue structure–property relationships.[11-16] In the early stage of nonlinear optics, NLO studies were focused mainly on inorganic materials, but in the 1970s a novel molecular engineering approach to optimize NLO effects in organic materials was proposed by Davydov et al.[17-19] It was found that strong second-harmonic generation is displayed by compounds having electron-donor and electron-acceptor groups attached to a benzene ring (Fig. 1a). This turning point aroused interest in searching for new conjugated organic molecules possessing large second-order optical nonlinearities. Today, the list of organic NLO molecules encompasses a broad range of donor–acceptor derivatives of benzene, stilbene and other analogous systems. In 1976, Sauteret et al.[20] found large third-order optical nonlinearity in polydiacetylene-p-toluene sulphonate; this opened new opportunities for studying conjugated organic polymers such as polyacetylene, polythiophenes, poly(p-phenylene vinylene), etc. Present research activities, therefore, have been proceeding toward an understanding and development of second-order and third-order NLO organic materials. In addition, there is a great deal of emphasis on development of new NLO devices using organic materials. Organometallics have also been recognized as playing a major role in the new emerging opto-electronic technologies and this review focuses on them.

2 NONLINEAR OPTICAL PHENOMENA

A laser is a source of light. The light emitted by a laser has a very high degree of collimation and coherence. Also, laser light is highly monochromatic and can be focused to a minimum spot size. Therefore a focused laser beam can provide a high power per unit area. The electromagnetic field of a light beam (laser), when directed on a material, generates an electrical polarization. For weak electric fields,[21] the polarization P is linearly proportional to the applied electric field E, which can be expressed by:

$$P = \varepsilon_0 \chi^{(1)} E \qquad [1]$$

In this equation, $\chi^{(1)}$ is the linear optical susceptibility and ε_0 is the permittivity of free space ($\sim 8.85 \times 10^{-14}\,\mathrm{F\,cm^{-1}}$). The susceptibility $\chi^{(1)}$ is related to the index of refraction of a material (n) by $\chi^{(1)} = n^2 - 1$; it is a tensor which follows the symmetry properties of the crystal. This is termed linear optics.

In the presence of a high optical field (e.g. the electromagnetic field of a laser beam), the induced polarization P in a macroscopic medium can be written as a power series of the applied field E (Eqn [2]):[22]

$$P = \chi^{(1)}.E + \chi^{(2)}.EE + \chi^{(3)}.EEE + \cdots \qquad [2]$$

where $\chi^{(2)}$ and $\chi^{(3)}$ are the second-order and third-order nonlinear susceptibilities; $\chi^{(2)}$ gives rise to second-harmonic generation (SHG) whereas $\chi^{(3)}$ causes third-harmonic generation (THG), and there are in addition a few other optical phenomena which arise from these two effects. Since $\chi^{(n)}$ are tensor quantities, the orientations of the molecules in a crystal lattice are important factors. If the molecular assembly has a centre of symmetry, $\chi^{(2)}$ is zero. Molecular assemblies that lack a centre of symmetry can exhibit second-harmonic generation. Like $\chi^{(1)}$, $\chi^{(2)}$ must also follow the symmetry properties of the crystal. Contrary to $\chi^{(2)}$ effects, there are no symmetry restrictions for the occurrence of $\chi^{(3)}$ effects, which broadens the scope of $\chi^{(3)}$ studies over a very wide variety of materials. Second-order and third-order nonlinear optical effects are correlated with quadratic hyperpolarizability β and cubic hyperpolarizability γ respectively. The polarization P induced in a molecule by an external electric field E can be written, analogously to Eqn [2], by the following relationship.[23,24]

$$P = \alpha.E + \beta..EE + \gamma...EEE + \ldots \qquad [3]$$

Hence, β and γ are measures of second-order and third-order NLO effects. For example, the value of β must be optimized in the case of SHG. Conjugated π-electron organic molecules containing electron-donor and electron-acceptor groups exhibit extremely large values of β.[25-27] Quadratic hyperpolarizability (β), which is the sum of two contributions, can be written as

$$\beta = \beta_{\mathrm{add}} + \beta_{\mathrm{CT}} \qquad [4]$$

where β_{add} is an additive term resulting from substituent-induced charge asymmetry and β_{CT} is

Table 1 Experimental values of β for organic molecules showing the influence of electron donor–acceptor groups and the conjugated system (data from Refs 28, 29)

| Molecule	$\beta_{exp}(10^{-30}\,esu)$
H$_2$N—◯	1.1
◯—NO$_2$	2.2
H$_2$N—◯—NO$_2$	34.5
(CH$_3$)$_2$N—◯—NO$_2$	220
H$_2$N—◯—◯—NO$_2$	260
(CH$_3$)$_2$N—◯—◯—NO$_2$	450
(CH$_3$)$_2$N—◯—NO$_2$	650

the charge transfer term related to transitions from the molecule's ground state to an excited state, induced by electromagnetic radiation (light). The β_{CT} term can be expressed in a two-level model (Eqn [5]) employed for organic molecules:[28, 29]

$$\beta_{CT} = \frac{3e^2h^2}{2m} \cdot \frac{W}{[W^2-(2h\omega)^2(W^2-(h\omega)^2]} \cdot f\Delta\mu \quad [5]$$

where e is the electronic charge, m is the mass, $h\omega$ is the fundamental photon energy, W is the energy of the optical transition, f is the oscillator strength of transition, and $\Delta\mu$ is the difference between excited-state and ground-state dipole moments. Therefore, in order to optimize β, both $\Delta\mu$ and f should be quite large. This objective can be accomplished by enhancing the electron-donating and electron-withdrawing activities of the donor and acceptor substituents separated by a conjugated π-electron system. Table 1 lists the experimental values of β for highly polar aromatic compounds of benzene and stilbene.[28, 29] Among o-, m- and p-nitroaniline isomers, the β value is much larger for p-nitroaniline (which has a donor and an acceptor group at the opposite ends) because of the increased intramolecular charge transfer between the substituents. Also, the β value increases as the conjugation length of the

system increases. In particular, a very large β value is generally exhibited by large conjugated molecules in which both a donor and an acceptor group interact in a mesomeric fashion. Figure 1 shows the molecular structures of the ground state and resonance excited state for p-nitroaniline (p-NA) and 4-dimethylamino-4'-nitrostilbene (DANS). The essence of the β and γ studies provides at least some first-hand primary information that assists in designing new organic molecules with large NLO properties.

There are a number of experimental techniques which have been used for the measurements of $\chi^{(2)}$ and $\chi^{(3)}$ effects; only some of the important ones are mentioned here. In 1968, Kurtz and Perry[30] developed a convenient and fast experimental technique for diagnosing SHG of powdered samples. The magnitude of SH intensity $I^{2\omega}$ yielded from a powder is compared with the SH intensity of powdered standard materials such as quartz, urea, etc., and this cross-check furnishes a rough estimate owing to the particle size dependence. The method of Maker fringes[5] is one of the most versatile techniques for determining SHG tensor elements (d coefficients). SHG coefficients are evaluated relative to those of standard materials [e.g. quartz (SiO$_2$), potassium dihydrogen phosphate, KDP (KH$_2$PO$_4$)]. SHG coefficients can also be determined by a phase-matching technique.[31, 32] Besides these, there are other methods to measure SHG coefficients.[33, 34] For third-order NLO effects measurement techniques such as third-harmonic generation (THG), degenerate four-wave mixing (DFWM), optical Kerr gate, self-focussing, electric field-induced
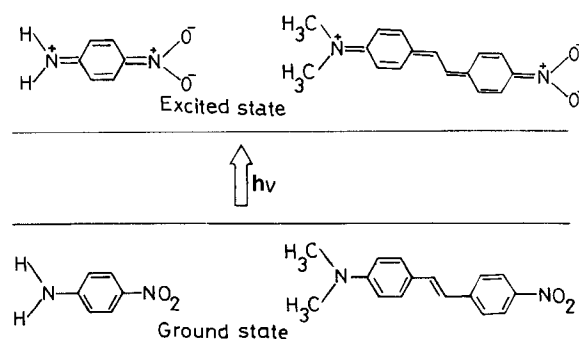
Figure 1 Molecular structures of the ground state and lowest-energy excited states for p-nitroaniline and 4-dimethylamino-4'-nitrostilbene. The amino (NH$_2$) and dimethylamino [N(CH$_3$)$_2$] are the electron-donating groups and nitro (NO$_2$) is an electron-withdrawing group.

$(pm/V)^2$

```
MNA  ─╆10⁴
 Te  ─╊
 NPP ─╊
MMONS ─╊10³
 DAN ─╊
  Se ─╊
COANP ─╊10²
 mNA ─╊
 MAP ─╊
Ba₂NaNb₅O₁₅,POM ─╊10
       HIO₃ ─╊
     LiNbO₃ ─╊
       ZnS ─╊
             ╊1
     UREA ─╊
 NH₄H₂PO₄ ─╊10⁻¹
    KH₂PO₄ ─╊
      SiO₂ ─╊
             ╊10⁻²
```
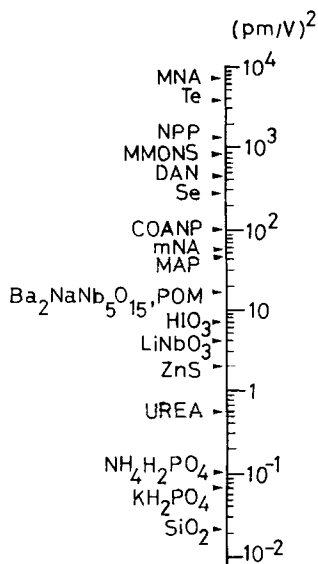
Figure 2 Nonlinear figure of merit for various inorganic and organic materials $[M = (d^2/n^3)]$. Measurement wavelength is $10.6\,\mu m$ for Te and Se, $1.06\,\mu m$ for other materials. Abbreviations: MNA, 2-methyl-4-nitroaniline; NPP, N-(4-nitrophenyl)-L-prolinol; m-NA, m-nitroaniline; COANP, 2-Cyclo-octylamino-5-nitropyridine; MAP, 3-methyl(2,4-dinitrophenyl)aminopropanoate; POM, 3-methyl-4-nitropyridine-1-oxide; MMONS = 3-methyl-4-methoxy-4'-nitrostilbene; DAN = 4(N,N-dimethylamino)-3-acetamido-nitrobenzene. (Adapted from Ref. 68.)

second-harmonic generation (EFISH), etc., have been used, for other methods readers are referred to the literature.[35-38]

3 NONLINEAR OPTICAL MATERIALS

A very large number of inorganic materials have been investigated in connection with nonlinear optics. A few typical examples of inorganic NLO materials of interest are: $LiNbO_3$, $KTiOPO_4$ (KTP), $Ba_2NaNb_5O_{15}$, $NH_4H_2PO_4$ (ADP), KH_2PO_4 (KDP), HIO_3, β-BaB_2O_4, LiB_2O_5, $CdGeAs_2$,$AgGaSe_2$, GaAS, $ZnGeP_2$, CdSe, Te and SiO_2 (quartz) (Fig. 2). Table 2 summarizes the nonlinear optical susceptibility, transparency range and damage threshold of a few of these important materials. Despite the moderate level of laser damage threshold ($\sim$100 MW cm^{-2}) for $LiNbO_3$ and KTP, they are promising for NLO devices (i.e. parametric oscillator, modulators, optical switches, etc.).[46] β-BaB_2O_4 manifests as a

suitable ultraviolet NLO crystal because of its high damage threshold and large SHG coefficient.[44] $CdGeAs_2$ and $AgGaSe_2$ are considered adequate as infrared NLO crystals, but they suffer due to their low damage threshold ($\sim$10 MW cm^{-2}) and poor optical quality.[47] Since 1963, numerous monographs and review articles have been published on various aspects of non-linear optics[48-52] and on inorganic NLO materials[53-57] which provide more details of these aspects.

Recently, research activities have been directed towards developing new organic molecular and polymeric NLO systems. The superiority of organic NLO materials has been valued because of their versatility and for the possibility of tailoring materials for particular end-uses. Organic NLO materials offer several advantages over inorganic NLO materials:

(i)   they exhibit large nonlinear figures of merit;
(ii) they sustain high optical damage thresholds (GW cm^{-2});
(iii) they show fast response times (sub-picoseconds);
(iv) they can be easily obtained in the form of ultrathin films, fibres, and even liquid crystals;
(v)   their architectural flexibility facilitates easy control of physical properties over a very wide range.

Compared with inorganic materials, the drawbacks of organic NLO materials are their moderate environmental stability, low mechanical strength and a limited temperature range of operation. Table 3 lists organic compounds with large second-order NLO properties. Umegaki[68] compiled nonlinear figures of merit of a wide variety of inorganic and organic materials. Figure 2 presents only some important materials. Nonlinear figures of merit d^2n^{-3} (where d is the nonlinear coefficient and n is the index of refraction) of MMONS,[67] DAN,[69] 2-cyclo-octylamino-5-nitropyridine COANP,[70] and 2-methyl-4-nitro-N-methylaniline (MNMA)[71] are 850, 420, 100 and 26 pm^2 V^{-2} respectively (see Table 3 for acronyms). In comparison with inorganic materials, the figures of merit of organic NLO materials are quite large. For example, MNA has a figure of merit 2000 times larger than that of $LiNbO_3$.[60] Although p-nitroaniline has a large β value, it has a centre of symmetry; hence second-order non-linearity vanishes (zero). Broadly speaking, the

majority of organic molecules (~70%) crystallize in centrosymmetric space groups[72] and therefore fail to exhibit SHG activity. Taking into account this situation, several strategies for forming acentric crystals capable of exhibiting SHG have been proposed: (i) chirality;[63,64] (ii) hydrogen bonding,[63,73] (iii) steric hinderance;[60] (iv) Langmuir–Blodgett technique;[74–76] (v) guest–host systems;[77–79] (vi) electrical poling;[80] (vii) co-crystallization;[81] (viii) a crystal growth technique;[82] (ix) channel inclusion alignment;[83] (x) lambda (λ)-type molecules,[84] (xi) dipole–dipole interaction reduction.[65] These methods have been found useful for ensuring a dipolar alignment favourable for exhibiting SHG activity. Organometallics have also been considered as a solution to this problem because of the extensively available combinations of a very wide variety of metals and organic ligands could introduce a chiral centre.

SHG studies on organic materials have been performed on single crystals, Langmuir–Blodgett films, NLO dye-functionalized polymer films, liquid crystals, guest (NLO dye)–host (polymer matrix) systems and polymers. Obviously, large SHG activity can be observed in organic single crystals because of high molecular density and uniformity, but high optical quality, large size, mechanically strong and defect-free crystals are required for fabricating NLO devices. Langmuir–Blodgett films, though formed in a very sophisticated technique to control

noncentrosymmetry and deposition of multi-layers, involves a rather time-consuming and tedious process. The guest–host system assures display of SHG, but SHG decreases due to the orientational relaxation and segregation. An alternative parallel to this is NLO dye-grafted polymers which show better stability as a function of time and also allow incorporation of high concentrations of NLO dye. In addition, material processability and fabrication into thin films make NLO dye-grafted polymers more interesting. In particular, poly(methyl methacrylate) and poly-styrene backbones have been used for grafting side-chain NLO dyes, since these polymers can provide transparency to the system.

Since a large number of NLO processes exist, therefore, requirement of an individual NLO material is confined to a particular application. For example, single crystals are promising for frequency conversion, while NLO dye-grafted polymers seem suitable for waveguides, etc. However, materials required for the design of NLO devices must fulfil certain basic conditions:

(i)   large nonlinear figures of merit;
(ii) appropriate transparency range;
(iii) high resistance to optical damage;
(iv) adequate birefringence for phase matching; and
(v)   good environmental stability.

These physical parameters help in evaluating the merit of NLO materials for applications. Organic

Table 2 Second-order nonlinear susceptibility,* transmission range and damage threshold of some important inorganic materials
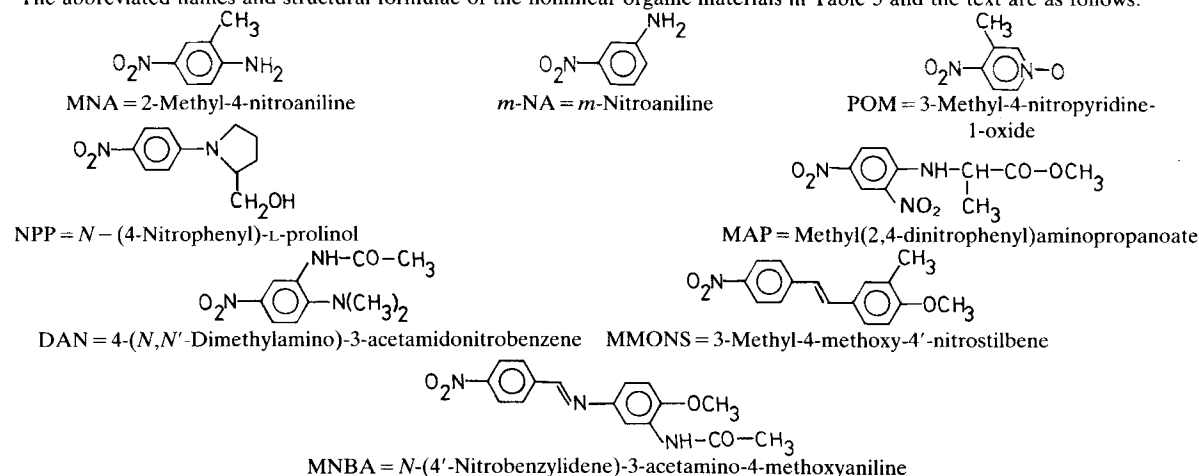
Material	SHG coefficient ($\times 10^{-9}$ esu)	Transmission range (μm)	Damage threshold (GW cm^{-2})	Reference
LiNbO$_3$	$d_{15} = 13$ $d_{22} = 6.6$	0.40–5.00	0.1 (1.064 μm, 12 ns)	39
KTiOPO$_4$ (KTP)	$d_{15} = 1.7$ $d_{31} = 6.5$ $d_{33} = 13.7$	0.35–4.50	0.16 (1.064 μm, 20 ns)	40, 41
NH$_4$H$_2$PO$_4$(ADP)	$d_{36} = 1.26$	0.19–1.20	0.5 (1.064 μm, 60 ns)	21
Ba$_2$NaNb$_5$O$_{15}$	$d_{15} = 31.3$ $d_{24} = 29.7$	0.38–6.00	0.01 (1.064 μm, 12 ns)	42
LiB$_2$O$_5$	$d_{31} = 2.75$ $d_{32} = 2.97$	0.16–2.60	25 (1.064 μm, 0.1 ns)	43
β-BaB$_2$O$_4$	$d_{11} = 4.1$	1.90–3.00	10 (0.694 μm, —)	44, 45
CdGeAs$_2$	$d_{36} = 560$ (10.6 μm)	2.40–18.0	0.04 (10.6 μm, 160 ns)	42
Te	$d_{11} = 1550$ (10.6 μm)	3.80–32.0	0.045 (10.6 μm, 190 ns)	42

* Second-order nonlinear susceptibility in pm V^{-1}; d_{ij} 1 pm V^{-1} = 2.387 $\times 10^{-9}$ esu
  Third order nonlinear susceptibility in m^2 V^{-2}; 1 m^2 V^{-2} = 0.716 $\times 10^8$ esu

Table 3 Second-order nonlinear optical coefficients, refractive indices, transparency range and optical damage threshold of some well-known organic materials

Material[a]	Refractive indices Wavelength: 1.064 μm	0.532 μm	d coefficient (10^{-9} esu)	Space group	Transparency range (μm)	Optical damage threshold (wavelength, μm)	Reference
Urea	$n_0 = 1.477$ $n_e = 1.583$	$n_0 = 1.490$ $n_e = 1.596$	$d_{36} = 5.1$	$P\bar{4}2_1m$	0.21–1.4	5 GW cm^{-2} (1.064)	58, 59
MNA	$n_x = 1.8$ $n_y = 1.6$ $n_z = ?$	$n_x = 2.2$	$d_{11} = 600$ $d_{12} = 90$	Cc	0.48–2.0	200 MW cm^{-2} (1.064)	58, 60
m-NA	$n_x = 1.760$ $n_y = 1.720$ $n_z = 1.670$	$n_x = 1.766$ $n_y = 1.732$ $n_z = 1.678$	$d_{31} = 46.7$ $d_{32} = 4$ $d_{33} = 49$	$Pbc2_1$	0.5–2.0	200 MW cm^{-2} (1.064)	58, 61
NPP			$d_{21} = 197$ $d_{22} = 73$ $d_{eff} = 243$	$P2_1$	0.48–2.0	50 MW cm^{-2} (1.064)	58, 62, 63
MAP	$n_x = 1.507$ $n_y = 1.599$ $n_z = 1.843$	$n_x = 1.556$ $n_y = 1.710$ $n_z = 2.035$	$d_{21} = 40$ $d_{22} = 44$ $d_{23} = 8.8$	$P2_1$	0.5–2.5	3 GW cm^{-2} (1.064)	58, 64
POM	$n_x = 1.663$ $n_y = 1.829$ $n_z = 1.625$	$n_x = 1.750$ $n_y = 1.997$ $n_z = 1.660$	$d_{14} = d_{25} = d_{36}$ $= 23$	$P2_12_12_1$	0.5–1.7	2 GW cm^{-2} (1.064) 150 MW cm^{-2} (0.532)	58, 65
DAN	$n_x = 1.517$ $n_y = 1.636$ $n_z = 1.843$	$n_x = 1.554$ $n_y = 1.732$ $n_z = 21.07$	$d_{22} = 12.4$ $d_{23} = 119$	$P2_1$	0.48–2.2	5 GW cm^{-2} (1.064)	66
MMONS	$n_x = 1.530$ $n_y = 1.630$ $n_z = 1.961$		$d_{24} = 170$ $d_{32} = 98$ $d_{33} = 440$	$Aba2$	0.51–2.1		67a
MNBA	$n = 1.901$	$n = 2.164$	$d_{11} = 1080$	Cc	0.50–2.0		67b

[a]The abbreviated names and structural formulae of the nonlinear organic materials in Table 3 and the text are as follows.

MNA = 2-Methyl-4-nitroaniline

m-NA = m-Nitroaniline

POM = 3-Methyl-4-nitropyridine-1-oxide

NPP = N – (4-Nitrophenyl)-L-prolinol

MAP = Methyl(2,4-dinitrophenyl)aminopropanoate

DAN = 4-(N,N'-Dimethylamino)-3-acetamidonitrobenzene

MMONS = 3-Methyl-4-methoxy-4'-nitrostilbene

MNBA = N-(4'-Nitrobenzylidene)-3-acetamino-4-methoxyaniline

NLO materials, as well as fundamental aspects related to them, have been reviewed by Zyss,[59] Williams,[27] Tripathy,[85] Flytzanis and Oudar,[86] Chemla and Zyss,[87] and Meredith.[88] Recently Nalwa et al.[89] have written a monograph describing in detail comprehensive studies on new organic materials as well as on measurement techniques applicable for second-harmonic generation. Several conference proceedings have been compiled on NLO processes and materials.[90–94] In addition, the Society of Photo-optical Instrumentation Engineers (SPIE) annually pub-

lishes conference proceedings on NLO processes and materials.

Despite considerable interest in organometallic NLO materials, there is no review literature on the important aspects of NLO properties of organometallics. This review attempts to highlight progress made in the development and evaluation of organometallics for NLO processes since their discovery in 1986. The present article is the first in-depth presentation of recent research information to investigators concerned with organometallic NLO materials. This review is intended to encourage organometallic chemists to design structurally and to synthesize new materials of interest. In particular, discussions will be focused on second- and third-order NLO properties of organometallics. In addition, the potential of organometallics in NLO devices will be presented.

3.1 Reasons for the proposed uses of organometallics for nonlinear optics

Metals that form chemical bonds with carbon are less electronegative than carbon itself. Carbon has an electronegativity value of 2.5, whereas the electronegativities of metals are much smaller. The nature of the metal–carbon (M–C) bond depends upon the electronegativity of an individual metal itself. For example, a potassium–carbon bond is highly ionic, whilst a cadmium–carbon bond is primarily covalent. Ligands attached to the metal atom also influence the nature of the metal–carbon bond. Electron-withdrawing ligands coordinated to the metal increase the electronegativity of the metal; on the other hand, electron-donating ligands decrease the electronegativity of the metal atom. Large differences in the electronegativities of metal and carbon atoms assist in introducing large polarities in organometallic compounds. Even greater intramolecular interactions are expected in organometallics that possess conjugated ligands because of the effective overlapping of the π-electron orbitals of ligands with the metal ion π-orbitals. An apparent feature that distinguishes organometallics from most organic systems is the charge-transfer transition. Organometallics have two kinds of charge-transfer transition, i.e. metal-to-ligand and ligand-to-metal. Many organometallics have low-energy excited states which help in reordering of the π-electron distribution.[95] Viewing organometallics through a two-level model (Eqn [5] above) suggests that they should

possess large NLO properties because of the large difference in the excited-state and ground-state dipole moments ($\Delta\mu$), and large oscillator strength (f) due to transfer of electron density between metal ions and ligands.[96]

In organometallics, a central metal atom can coordinate to different ligands. A wide variety of central metal atoms (and also their size, nature, and oxidation states), as well as the size and nature of the ligands, provides architectural flexibility to tailor NLO properties up to a maximum level. As discussed earlier, a noncentrosymmetric structure is required for second-order NLO effects; coordination of a central metal ion with different ligands could introduce a chiral centre in an organometallic molecule and therefore a high percentage of organometallic compounds are expected to have acentric crystal structures. Keeping these important points in mind, the potential of organometallic compounds has been accepted for nonlinear optics.

4 SECOND-ORDER NONLINEAR OPTICS IN ORGANOMETALLIC COMPOUNDS

4.1 Ferrocene derivatives

The first report on the NLO properties of a ferrocene derivative appeared in 1987. Green et al.[97] reported the synthesis and structure of cis-[1-ferrocenyl-2-(4-nitrophenyl)ethylene] [$(\eta$-$C_5H_5)Fe(\eta$-$C_5H_4)CH = CH$—p-$C_6H_4NO_2$]. The dark purple crystals of the cis-isomer crystallize in a noncentrosymmetric space group Cc, whereas its counterpart, the trans-isomer, has a centre of symmetry and hence exhibits no SHG signal. The cis-isomer shows interesting solvatochromic behaviour, i.e. three absorptions (at 320, 406, and 462 nm) occur in heptane, whilst only two absorptions (at 340 and 492 nm) occur in N,N'-dimethylformamide. Kurtz powder measurements at 1.064 μm give SHG efficiency as high as 62 times that of a urea reference sample for cis-[1-ferrocenyl-2-(4-nitrophenyl)ethylene].[97] It has been suggested that this large second-order optical nonlinearity appears from the interesting redox nature of the ferrocene derivatives. A large molecular second-order hyperpolarizability occurs due to the charge-transfer characteristics and the π-electron conjugation system.

Bandy et al.[98] reported second-order optical nonlinearities of a series of ferrocenyl compounds. The compounds of general formula (η -C_5H_5)Fe(η-C_5H_4)CH=CHR, where R refers to p-C_6H_4—NO_2, —p-C_6H_4—CN, —p-C_6H_4—CHO, —(E)-CH=CH—p-C_6H_4—NO_2 and —C̿=CH—CH=C(NO_2)O, exhibit powder SHG efficiencies of 8.0, 1.2, 2.5, 6.4 and 17.0 times that of urea respectively. The SHG efficiencies are sensitive to the enantiomeric ratio. Ferrocenyl-ethylene complexes containing 82% enantiomeric excess of the s-isomer show large SHG efficiencies.

Recently, Marder et al.[99] synthesized ferrocene derivatives having general formula (E)-(η-C_5H_5)Fe   (η-C_5H_4)—CH=CH-p— ($C_5H_4NCH_3$)$^+X^-$, where X^- refers to a counterion (Fig. 3). A series of organometallic salts having counterions I^-, Br^-, Cl^-, $CF_3SO_3^-$, BF_4^-, PF_6^-, p-$CH_3C_6H_4SO_3^-$, NO_3^- and $B(C_6H_5)_4^-$ were prepared and their SHG efficiencies were examined by a modified Kurtz powder technique at 1.907 μm.

Interestingly, a significant effect of the incorporated counterion variation has been observed. Organometallic salts having counterions I^-, Br^-, NO_3^-, BF_4^-, and p-$CH_3C_6H_4SO_3^-$ show SHG efficiencies of 220, 170, 75, 50 and 13 times that of a urea standard, respectively. The PF_6^- salt has a small relative SHG efficiency of 0.05, whereas no SHG signal was detected for Cl^- and $CF_3SO_3^-$ counterions. The $B(C_6H_5)_4^-$ counterion salt exhibits an SHG efficiency 13 times that of urea, the same as that of the p-$CH_3C_6H_4SO_3^-$ salt.

Recently, Cheng et al.[100] measured molecular hyperpolarizabilities (β) of ferrocene and ruthenocene derivatives (Fig. 4). Ferrocenes such as trans-(η-C_5H_5)Fe(η-C_5H_5),   [η-$C_5(CH_3)_5$]Fe(η-C_5H_5), [η-$C_5(CH_3)_5$]Fe(η-C_5H_4)CN) have β values of 31.0 × 10^{-30}, 40.0 × 10^{-30} and 35 × 10^{-30} esu respectively. A ferrocene derivative [(η-C_5H_5) Fe(η-C_5H_4)COCH$_3$] shows a β value of about 0.3 × 10^{-30} esu. The coupling of the ferrocene moiety with a 4-nitrophenylvinyl group as well as other structural changes affect the nonlinear optical responses. For example, 2,4-dinitro- and 4-nitrophenyl-butadiene–ferrocene show very
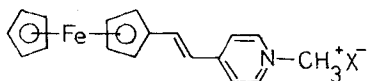

Figure 3 Chemical structure of a ferrocene derivatized salt (after Ref. 99).
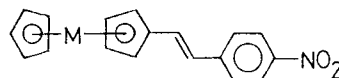

Figure 4 Chemical structure of a metallocene complex (after Ref. 100).

large β values of 23 × 10^{-30} and 66 × 10^{-30} esu respectively, which are in the range of the well-known nitrostilbene derivatives. On the other hand, ruthenocene (η-C_5H_5)Ru(η-C_5H_5), [η-$C_5(CH_3)_5$]Ru(η-C_5H_5) and [η-$C_5(CH_3)_5$]Ru(η-C_5H_4)CN exhibit β values of 12 × 10^{-30}, 24 × 10^{-30} and 24 × 10^{-30} esu respectively. Both in ferrocene as well as in ruthenocene, substitution of penta-methyl groups leads to an increase in β values. The nonlinearity of ferrocene compounds is larger than that of analogous ruthenocenes, which probably results from the difference in oxidation potentials.

4.2 Metal carbonyl complexes

Frazier et al.[96] evaluated SHG efficiencies of about 60 transition-metal organic complexes of Group VI metal carbonyl arene, pyridyl and chiral phosphine complexes. The arene Group VI metal carbonyl complexes have a general formula $M(CO)_nL_{3-n}$, where M is a Group VI transition metal (Cr, Mo, W), L is a phosphine ligand, and n = 0, 1, 2 or 3. An arene is for example a benzene ring. The arene carbonyl chromium(0) complexes show SHG efficiencies from 0.01 to 1.8 times that of ammonium dihydrogen phosphate (ADP). The Cr(S)-(+)-(2-methylbutyl)benzene(CO)$_3$ and Cr(styrene)(CO)$_3$ complexes whose structures are depicted in Fig. 5 have the largest SHG efficiencies of 1.7 and 1.8 times that of ADP respectively. It has been found that electron-withdrawing groups close to the benzene ring leads to zero SHG efficiency. On the other hand, the metal atom interaction shows a positive effect. For example, the SHG efficiency of the Cr(L-phenyl-alanine ethyl ester hydrochloride) (CO)$_3$ complex is about 30 times larger than that of the corresponding parent compound. Pyridyl Group VI
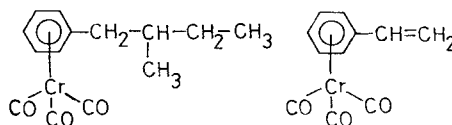

Figure 5 Chemical structures of arene chromium carbonyl complexes. [Reprinted with permission from J. Phys. Chem., 1986, 90: 5703, Frazier et al.[96] Copyright (1986) American Chemical Society.]
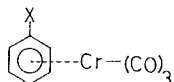
Figure 6 Chemical structure of π-CTCB complexes (after Ref. 100).

metal carbonyl complexes have a general formula $M(CO)_{5-n}L_n$(pyridyl group), where M is the transition metal (Cr, Mo, W), L is the phosphine ligand, and $n = 0$ or 1. In these complexes, pyridine is attached to the metal atom through the ring nitrogen atom. The SHG efficiencies of pyridyl carbonyl Group VI metal complexes are rather small, ranging between 0.04 to 1.0. Interestingly, one of the parent compounds (4-benzoylpyridine) has an SHG efficiency 14 times that of ADP. Its chromium and molybdenum complexes are SHG-inactive, while the tungsten complex [$W(CO)_5$(4-benzoylpyridine)] has a relative SHG value of 0.2.

The carbonyl transition-metal (Fe, Mo and W) complexes containing the neomenthyl diphenylphosphine ligand exhibit SHG efficiencies of 0.01 to 0.06 compared with a standard ADP sample. Although all of these complexes are SHG-active, the SHG signal is much smaller than that of the ligand itself. Among all these transition-metal complexes, arene tricarbonyl chromium(0) complexes show the largest SHG efficiencies and, to some extent, the SHG activity is also influenced by the nature and the presence of a particular transition-metal species.

Another miscellaneous transition-metal series of complexes which do not belong to either of above-mentioned classes was also studied by Frazier et al.[96] $Fe(CS_2)(CO)_2[P(OCH_3)_3]_2$, $Mo(CO)_4(PPh_3)_2$ and tris[3-(heptafluoropropyl-hydroxymethylene) - d - camphorato]praseodym - ium(III) have SHG efficiencies of 0.03, 0.01 and 0.2 times that of ADP respectively. Some of the carbonyl derivatives, such as $Fe(CS_2)$ $(CO)_2$ $[P(C_6H_{11})_3]_2$ and $Fe(CS_2)(CO)_2[P(OCH_3)_2Ph]_2$, and acetylferrocene and benzylferrocene were found to be SHG-inactive complexes.

Cheng et al.[100] measured second-order hyperpolarizability of chromium tricarbonyl benzene π-complexes (π-CTCB) in solution (Fig. 6). The π-CTCB complexes with substituent groups X = H, OCH_3, $COOCH_3$, NH_2 and $N(CH_3)_2$ show hyperpolarizability β values of -0.8×10^{-30}, -0.9×10^{-30}, -0.7×10^{-30}, -0.6×10^{-30} and -0.4×10^{-30} esu respectively. These results indicate that the β values of these π-CTCB complexes are not influenced by the electron affinities of the substituent groups since the metal donor group is not in conjugation with the benzene substituents. Furthermore, the β values have a negative sign. The electronic absorption studies suggest that the weak bathochromic shifts with electron-donating and -accepting substituent groups demonstrate poor charge-transfer interactions.

Nonlinear optical properties for the organometallic cluster compounds $HFeCo_3(CO)_{10}$-$[P(CH_3)]_2$ and $HFeCo_3(CO)_{10}[P(C_6H_5)_3]_2$ have recently been reported by Tutt et al.[101] Excited-state absorption measurements show that the excited state of both cluster compounds has a lifetime of 115 ns. The incorporation of these cluster compounds into poly(methyl methacrylate) matrices also produces optical limiting properties similar to the parent cluster compounds.

4.3 Metal pyridine and bipyridine complexes

Second-order NLO properties of pyridine (pyr) and bipyridine (bipyr) complexes of rhenium (Re), platinum (Pt), palladium (Pd), molybdenum (Mo), tungsten (W) and chromium (Cr) have been investigated by Calabrese and Tam.[102] The complexes $BrRe(pyr)_2(CO)_3$ and $BrRe(4-styrylpyridine)_2(CO)_3$ show SHG efficiencies in the range 0.1 to 0.2 relative to the reference urea sample. The $ClRe(bipyr)(CO)_3$ complex has SHG efficiency of the order of 1.6 to 3.0 times that of urea. The complexes of $Pt(bipyr)Cl_4$, $Pd(bipyr)Cl_4$, $Mo(bipyr)(CO)_4$, $W(bipyr)(CO)_4$ and $Cr(bipyr)(CO)_4$ have relative SHG efficiencies of 1.2, 0.1, 0.5, 0.3 and 0.2 times that of urea respectively. The yellow [$CF_3SO_3Re(2,2'$-bipyr)(CO)_3$] complex shows SHG efficiency in the range 1.7 to 2.0 relative to that of urea and this complex crystallizes in a noncentrosymmetric space group $P2_1$. Molecules of this complex form staggered chains along the 2_1 axis in the crystal; since they lack a centre of symmetry, they are SHG-active. All of the pyridine and bipyridine organometallic complexes have low-lying charge-transfer states and their SHG efficiencies range from 0.1 to 3.0 times that of urea.

Cheng et al.[100] report the second-order hyperpolarizability of tungsten pentacarbonyl pyridine σ-complexes (σ-TPCP) (Figure 7). These complexes have a σ-linkage since the nitrogen loan pair donates into the empty d-orbital (d_{zz}) of tungsten metal. The σ-TPCP complexes having

substituent groups X = H, C_6H_5, C_4H_9, NH_2, $COCH_3$, and CHO show β values of -4.4×10^{-30}, -4.5×10^{-30}, -3.4×10^{-30}, -2.1×10^{-30}, -9.3×10^{-30} and $+12.0 \times 10^{-30}$ esu respectively, indicating that β values are sensitive to substitution at the 4-position. *Para* substitution in conjugation with tungsten pentacarbonyl plays a significant role and these complexes have metal-to-ligand charge-transfer excitations.

4.4 Bimetallic complexes containing ferrocenyl and nitrosyl centres

The complexes [M(NO)LXY] {L = tris(3,5-dimethylpyrazolyl)borate [HB(Me$_2$Pz)$_3^-$]; M = Mo, W; X = I, Cl; Y = O, NH, OPh, NC_4H_4, NHPh, SPh, etc.} have been investigated by Briggs *et al.*[103] These 16-electron complexes have been of considerable interest for studying the effect of donor atoms on the reduction potentials. The 16-electron complex [M(NO)LClY] (Y = O, NH) acts as an electron-accepting species, whereas the 17-electron [M(NO)LClY]$^-$ moiety acts as an electron-donating species.[104, 105] The molybdenum and tungsten mononitrosyl complexes exhibit SHG intensities in the range 0.004–123 times that of a urea standard, as reported by Coe *et al.*[106] The complexes [Mo(NO)LX(−)-OCH$_2$CH (Me)C$_{10}$H$_6$OMe)] (X = Cl or I; C$_{10}$H$_6$ = naphthyl) show a very weak SHG signal (0.004–0.007 times that of urea). The complexes [Mo(NO)LCl(3-*o*-1,2:5,6-di-isopropylidene-*o*-D-glucofuranate] and W(NO)LCl [(*R*)-(+)-methylbenzamide)], containing chiral metal centres as well as chiral ligands, also show weak SHG. The complexes [M(NO)LCl(NHC$_6$H$_3$(3-Me)—4-N=N—C$_6$H$_4$—4'—Fc], where Fc refers to (η-C$_5$H$_5$)Fe(η-C$_5$H$_4$), show an SHG intensity 53 times that of urea for the tungsten complex, whilst the SHG intensity of the molybdenum complex is 2.32 times larger than that of the tungsten complex (i.e. 123 times that of urea for molybdenum). Surprisingly, in the corresponding iodine complex Mo(NO)LI-[NH—C$_6$H$_3$—(3-Me)—4-N=N—C$_6$H$_4$—Fc], the SHG intensity decreases to 0.12 times that of urea. A [Mo(NO)LCl(NH—C$_6$H$_4$—4-N=N—C$_6$H$_4$—4'—Fc) complex exhibits an SHG intensity 59 times that of urea. When the metal mononitrosyl acceptor group is replaced by NO$_2$C$_6$H$_4$—4-N=N—C$_6$H$_4$—4'-Fc or NO$_2$C$_6$H$_3$—

$$X—\langle N \rangle—W(CO)_5$$

Figure 7 Chemical structure of *o*-TPCP complexes.

Figure 8 Coordinate structure of thiocyanate double salts (after Ref. 107).

(3-Me)—4-N=N—C$_6$H$_4$—4'-Fc, neither of the complexes shows detectable SHG intensities. Also, the replacement of Fc by *trans*-1,2-ethenyl, OMe or NMe$_2$ groups gives compounds with little or no SHG activity, so it is probable that the C$_6$H$_4$—N=N—C$_6$H$_4$—Fc species plays a significant role in generating SHG in these bimetallic complexes.

4.5 Organometallic complexes of Thiourea and its derivatives

The complexes M(L)X$_2$, where M is cadmium (Cd), lead (Pb), mercury (Hg), iron (Fe), manganese (Mn) or zinc (Zn), L is thiourea (TU), allylthiourea (ATU) or thiosemicarbazide (TSC), and X is chlorine, bromine or iodine, have been investigated by Tao *et al.*[107, 108] The Cd(TU)$_2$Cl$_2$, Cd(ATU)$_3$Br$_2$ and Hg(ATU)$_3$Br$_2$ complexes show SHG intensities 100, 150 and 350 times that of a reference quartz sample, respectively. A Cd(TU)$_2$Cl$_2$ complex exhibits an SHG intensity as high as 700 times that of quartz (SiO$_2$). The M(TU)$_4$X$_2$ complexes, where M = Cd, Fe, Mn, Pb or Zn and X = Cl or Br, show no SHG activities. All of the thiocyanate double salts, M$_1$M$_2$(SCN)$_4$, are SHG-active (Fig. 8). The double salts of CdHg(SCN)$_4$, ZnHg(SCN)$_4$ and ZnCd(SCN)$_4$ have SHG intensities 600 times that of quartz. Another thiocyanate double salt, MnHg(SCN)$_4$, has an SHG intensity 400 times that of quartz. Organometallic salts with thiosemicarbazide and thiocyanate ligands such as Cd(TSC)(SCN)$_2$ and Zn(TSC)(SCN)$_2$ show SHG intensities of 140 and 80 times that of quartz respectively. A Cd(NH$_2$—NH–CS—NH$_2$)Cl$_2$.H$_2$O i.e. thiosemicarbazide cadmium chloride (TSCCC) complex that has a TSC bidentate ligand crystallizes into space group *Cc*. A heterocyclic conjugated system is formed in this complex by the sulphur and amino nitrogen atoms via coordination with the central cadmium ion. The refractive indices n_x, n_y and n_z of TSCCC at 0.532 μm are 1.67829, 1.75161 and 1.77660, while at 1.064 μm they are 1.64950, 1.75161 and 1.77660 respectively. The NLO $d_{effective}$ coefficient of TSCCC is 5.2 times the d_{36} of a KDP crystal. These thiourea-derivative organometallic complexes seem quite interesting

because of their ease of synthesis and large SHG efficiencies.

Recently, Zhang et al.[108] reported the nonlinear optical properties of the organometallic complex triallylthiourea cadmium chloride [CdCl(CH$_2$= CHCH$_2$NHCSNH$_2$)$_3$$^+Cl^-$] (ATCC). ATCC single crystals of dimensions as large as 30 mm × 30 mm × 25 mm can be obtained. ATCC belongs to the noncentrosymmetric space group R_{3c}, point group C_{3v}. The unit cell parameters are $a = b = 11.527(4)$ Å, $c = 27.992(6)$ Å. The density is 1.63 g cm^{-3}. After Kleinman symmetry relations, only three independent tensor elements remain, i.e., $d_{15} = d_{31}$, d_{22} and d_{33}. These nonlinear coefficients measured by the Maker fringe method correspond to $d_{22} = 0.7 \times 10^{-9}$, $d_{31} = 1.5 \times 10^{-9}$, and $d_{33} = 1.9 \times 10^{-9}$ esu. ATCC shows an optical damage threshold of 320 MW cm^{-2} for a 10 ns laser pulse width. In ATCC, the optimum second-harmonic generation is observed with an angle of incidence of 36.8°. The ultraviolet cut-off wavelength is about 300 nm. Tri-allylthiourea cadmium bromide (ATCB) belongs to space group R_{3c} and has transparency 0.3–1.5 μm. It shows SHG efficiency 1.5 times that of urea. Another thiourea complex namely thiosemicarbazide cadmium thiocyanate (TSCCTC) belonging to space group $P2_12_12_1$ shows d_{14} of 1.52×10^{-9} esu.[109]

4.6 Channel inclusion complexation of organometallics

Eaton et al.[83] report that guest–host inclusion chemistry provides a new avenue for forming noncentrosymmetric crystal structures for SHG. Inclusion hosts such as thiourea, tris-o-thymotide, deoxycholic acid and clathrate hosts (e.g. cyclodextrins) form polar guest–host inclusion complexes with organometallics. Host–guest inclusion complexes having 1:1 to 1:3 host–guest ratios show SHG intensities in the range 0.1 to 2.3 times that of urea. Out of the inclusion complexes that were investigated for thioruea, tris-o-thymotide ligands and organometallics, nearly 60% are SHG-active. In particular, 3:1 thiourea-to-organometallic inclusion complexes mostly crystallize in noncentrosymmetric space groups. A 3:1 thiourea-to-(η-C$_6$H$_6$)Cr(CO)$_3$ inclusion complex shows SHG intensity 2.3 times that of urea. The benzene ligands can be replaced by pyrrole, thiophene, diene and carbonyl (CO) ligands as well as by ferrocene.

Among thiourea organometallic inclusion complexes, 69% are SHG active, while for tris-o-

thymotide, only 50% are SHG-active. The authors suggested that if the channel dimensions are maintained smaller than the guest dimensions, then head-to-tail dipolar orientation by the guests is achieved along the channel directions. In cases where the channel dimensions are larger than optimal, dipolar orientation is difficult.[110] Also, dipolar arrangement may not occur if hydrogen bonding and π–π interactions of aromatic rings exist in the inclusion complexes. The thiourea inclusion complexes of (η-C$_6$H$_6$)Cr(CO)$_3$ and (η^4-trimethylenemethane)Fe(CO)$_3$ have SHG intensities of 2.3 and 0.3 respectively and crystallize in the space group $R3c$, whilst (η-1,3-cyclohexadiene)Fe(CO)$_3$ has an SHG intensity of 1.0 and crystallizes in the space group $Pna2_1$.

4.7 Miscellaneous organometallics

The reaction of ruthenium (η-cyclopentadienyl)bis(triphenyl phosphine) chloride, (η-C$_5$H$_5$)Ru(Ph$_3$P)$_2$Cl with 4-cyano-4'-n-pentyl-p-terphenyl and ammonium hexafluorophosphate in methanol yields pale yellow crystals of ruthenium(η^5-cyclopentadienyl)bis(triphenyl phosphine)-4-cyano-4'-n-pentyl-p-terphenyl hexafluorophosphate (RuCTP).[111] In RuCTP (Fig. 9) the ruthenium (η^5-cyclopentadienyl)bis(triphenylphosphine) moiety is hydrophilic, whereas n-pentyl-p-terphenyl is hydrophobic. Therefore, as a result, this molecule forms Langmuir–Blodgett films. The cyano group that bridges the hydrophilic and hydrophobic units also contributes in enhancing the electron-withdrawing activity; hence it assists in increasing the molecular hyperpolarizability.[111] Langmuir–Blodgett (LB) monolayer formation indicates that the RuCTP molecule occupies a surface area of 157.0 Å^2 per molecule. RuCTP exhibits molecular hyperpolarizability about one-half that of hemicyanine. The second-harmonic signal intensity, though, increases as the square of the number of RuCTP layers, but it deviates from the square law indicating that the molecular alignment changes from one layer to the other.

Square-planar platinum and palladium benzene complexes having general formula MXL$_2$Y, where M = Pt and Pd, X = bromine and iodine,
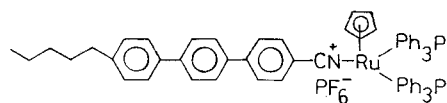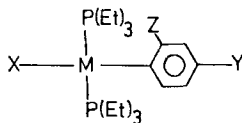

Figure 9 Structure of RuCTP (after Ref. 111).

Figure 10 Structure of platinum and palladium complexes.

$L_2 = [P(C_2H_5)_3]_2$ and $Y = NO_2$ and CHO, have been investigated by Cheng *et al.*[100] In these complexes, the parent compounds MXL_2 act as electron donors and NO_2 and CHO are electron acceptors. Bromo ligand compounds have larger nonlinearity than iodo complexes. Also, the *p*-nitrophenyl derivative shows a larger β value than the *p*-benzaldehyde derivative, indicating that the strong electron acceptor group is more effective. A $PtBr_2[P(C_2H_5)_3]_2$-*p*-nitrobenzene complex exhibits a β value as high as 3.8×10^{-30} esu.

Tam *et al.*[112] previously reported the second-harmonic generation of platinum and palladium complexes of aromatic halides having general formula $M(PEt_3)_2(X)(2-Z-4-Y—C_6H_4)$, where $X = Br$, I; $Z = H$, CH_3, NO_2; $Y = H$, CHO, NO_2, CN (Fig. 10). The $M(PEt_3)_2(X)$ moiety acts as a donor in aromatic donor–acceptor compounds. All of these organometallics are air-stable. The powder SHG efficiency of these organometallics measured at $1.064\,\mu m$ ranges from 0.4 to 14 times that of urea. The powder SHG efficiency changes with particle size. A $Pt(PEt_3)_2(Br)(2-CH_3-4-NO_2—C_6H_4)$ compound shows the largest SHG efficiency (14 times that of urea). The SHG efficiency of $Pd(PEt_3)_2(Br)(2-CH_3-4-NO_2—C_6H_4)$ compound ranges from 5 to 10. The SHG efficiency of these organometallics are affected by the substituents on the phenyl ring, the nature of the metal atom and the halogens.

Kanis *et al.*[113] calculated the second-order hyperpolarizabilities of transition-metal organometallic chromophores using a self-consistent field (SCF) linear combination of atomic orbitals (LCAO) mono-excitation configuration interaction (MECI) approach. The hyperpolarizabilities of organometallic complexes $(\eta$-$C_5R_5)Fe(\eta$-$C_5H_4)CH=CX—C_6H_4—NO_2$, where $R = H$, CH_3 and $X = H$, CN (the structure is given in Ref. 100), $W(CO)_5(NC_5H_4R)$ where $R = H$, NH_2, phenyl, $COCH_3$ and n-butyl (structure is shown in Ref. 100) and $Cr(styrene)(CO)_3$·complexes having H, NH_2, OCH_3, $COOCH_3$, $N(CH_3)_2$ and *trans*-styryl substituents on the benzene ring (structure in Ref. 96) have been calculated theoretically and compared with experimental values. The molecular hyperpolarizabilities of these

organometallics are greatly affected by the substituents, and metal *d–d* transitions play very little role. In particular, hyperpolarizability is increased by the substituents that increase the donor characteristics of the ferrocenyl group.

Chollet *et al.*[114] reported second-harmonic generation in vacuum-deposited copper phthalocyanine (CuPc) films of thickness ranging from 50 to 500 nm. The CuPc films show incident angle dependence of the SHG signal, a characteristic that has been often observed in oriented LB films and also in electrically poled polymer thin films. A 162 nm thick CuPc film exhibits d_{33} coefficients of 11.5×10^{-9} and 65×10^{-9} esu for *p–p* and *s–p* polarization configurations respectively. In this case, d_{33} values have been derived using the Langmuir–Blodgett (LB) film approach. On the other hand, d_{31} and d_{33} coefficients derived using an electrically poled polymer film approach correspond to 3.76×10^{-9} and 11.3×10^{-9} esu for *p–p* polarizations for a 78 nm thick film, whereas a 162 nm thick CuPc film shows a d_{31} coefficient of 11.4×10^{-9} esu for a *s–p* polarization and a d_{33} value of 31×10^{-9} esu for *p–p* polarization. The d_{eff} of the CuPc film corresponds to between 30×10^{-9} and 60×10^{-9} esu. No SHG signal is observed for *p–s* and *s–s* polarizations. The origin of the non-zeroth second-order nonlinear susceptibility in CuPc thin film is quite surprising because the CuPc molecule should be centrosymmetric with zero second-order hyperpolarizability $(\beta = 0)$. The SHG signal displayed by the CuPc molecule may be of quadrupolar and/or dipolar origin. Electron spin resonance (ESR) experiments performed for various rotation angles of the CuPc sample demonstrate that the Pc rings lie almost parallel to the substrate plane, with a large angular distribution. The copper atoms probably remain outside the plane. Nalwa[115] first reported that a pristine CuPc sample displays pyroelectric current on heating and recorded the magnitude of current increases in electrically poled samples. The appearance of spontaneous polarization (i.e. in a pristine unpoled sample) in the CuPc molecule suggests that second-order nonlinear optical effects are true phenomena. Similar pyroelectric behaviour has been observed in other MPcs. Chollet *et al.*[114] reported that the metal-free (H_2Pc) and zinc-containing (ZnPc) phthalocyanines showed no SHG signal and this may further substantiate a role for the central metal atom for SHG activity.

Marder *et al.*[116] investigated the second-order optical nonlinearities of some linear donor–
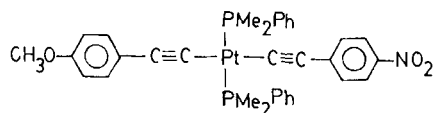
Figure 11 Chemical structure of linear donor–acceptor substituted platinum acetylide (after Ref. 116).

acceptor substituted transition-metal acetylide (Fig. 11). The *trans*-complex belongs to the space group $P1$ and there is one molecule per unit cell ($Z = 1$). The complex (Fig. 11) shows an absorption maximum at 386 nm and has an absorption coefficient (ε) of 38 800. The powder sample is SHG active (about equal to that of quartz). Other unsymmetrical *trans*-bis(acetylide) complexes having donor alkynes such as 4-ethynylpyridine, ethynyl ferrocene and ethynyl diphenylphosphines and various diacetyline (—C≡C—C≡C—) units also exhibit SHG activity.

Thompson *et al.*[117] reported the nonlinear optical properties of monomeric, dimeric and trimeric titanium complexes based on $(C_5H_5)_2TiX_2$ (Fig. 12). In oligomeric complexes, $(\eta C_5H_5)_2Ti$
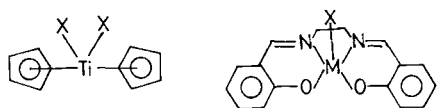
Figure 12 Chemical structures of (a) titanium complexes based on $(C_5H_5)_2TiX_2$ and (b) Salen coordination complexes (after Ref. 117).

units are joined together via —C≡C— linkages. A titanium acetylide polymer consisting of a highly delocalized π-electron system is expected to show large third-order hyperpolarizability (γ). The inorganic Salen coordination polymers of chromium(III), manganese(III) and iron(III) and cobalt(III) have square-pyramidal structures. These complexes have a general formula (Salen)MX, where Salen is a planar tetradentate dianionic ligand, M is the metal atom and X is the apical ligand of an adjacent molecule, through which metal complexes polymerize by coordination. Both polar and nonpolar complexes having metal atom acceptors and organic donors can be obtained. The colour of these materials ranges from orange to green, and polar molecules display an SHG at $1.064 \mu m$.

Recently Mignani *et al.*[118] reported the second-order NLO properties of a new class of silicon compounds which have high optical transparency. Table 4 lists the chemical structures, optical spectra and molecular hyperpolarizabilities of these silicon compounds. The compounds contain electron-donor and electron-acceptor groups separated by silicon atoms. The β measurements carried out by the electric field induced second-harmonic generation (EFISH) method show that the hyperpolarizability (β) of organosilicon compounds increases as the number of silicon (Si) atoms increases due to the delocalization of σ-electrons along the Si–Si backbone. The β value of compound C (Table 4) is about 3 times larger

Table 4 Molecular hyperpolarizability, absorption maxima and physical properties of silicon compounds containing electron-donor and electron-acceptor groups (after Ref. 118)

Silane[a]	Number of dimethylsilane units (n)	Melting point (°C) (Colour)	Absorption maximum in $CHCl_3$ (nm)	Hyperpolarizability β (10^{-30} esu)
A	1	— (Red oil)	320	16
B	2	98–100 (Yellow–orange)	334	22
C	6	138–139 (Yellow crystalline)	276	38

[a]A = [4-(2,2-Dicyanoethenyl)phenyl][4-(dimethylamino)phenyl]dimethylsilane
B = 1-[4-(2,2-Dicyanoethenyl)phenyl]-2-[4-(dimethylamino)phenyl]-1,1,2,2-tetramethyldisilane
C = 1-[4-(2,2-Dicyanoethenyl)phenyl]-6-[4-(dimethylamino)phenyl]-
1,1,2,2,3,3,4,4,5,5,6,6-dodecamethylhexasilane

than the β-value of p-nitroaniline (p-NA) Teng *et al.*[119] reported a β value of 8.4×10^{-30} esu for p-NA in dioxane ($\lambda_{max} = 354$ nm). These charge-transfer complexes of silicon show high transparency coupled with large molecular hyperpolarizability.

Recently Li *et al.*[120] utilized a self-assembly synthetic approach in building organic superlattice structures for nonlinear optics. These multi-layer structures contain silicon layers and poly(vinyl alcohol) layers which sandwich stilbazole chromophores. These hard multilayers are insoluble in organic solvents and strong acids. A superlattice thin film shows a $\chi^{(2)}$ value of 2×10^{-7} esu. The SHG efficiency of a five-layer superlattice structure decreases by about 10% over a period of a month. These self-assembled superlattice structures seems promising for nonlinear optics.

In 1982, Vizgert *et al.*[121] reported that lanthanide formate ($Ln(HCOO)_3$), which belongs to the space group $R3m$, shows a powder SHG efficiency equal to that of KDP (KH_2PO_4). The inorganic salts potassium-4-aminobenzene sulphonate ($H_2NC_6H_4SO_3K$) and sodium 3-nitrobenzene sulphonate ($O_2NC_6H_4SO_3Na$) also have the same magnitude of powder SHG as $Ln(HCOO)_3$. Yttrium formate dihydrate $[Y(HCOO)_3 . 2H_2O]$,[122] which belongs to the space group $P2_12_12_1$, and anhydrous yttrium formate $[Y(HCOO)_3]$[123], belonging to the space group $R3m$, have powder SHG efficiencies 0.5 and 2 times that of KDP respectively. Davydov *et al.*[124] reported that lithium vanillinate hydrate $[OH(CH_3CO)C_6H_4COOLi . nH_2O]$, sodium p-nitrophenolate hydrate ($NaOC_6H_4NO_2 . nH_2O$) and potassium L-aspartate $[HOOCCH_2CH(NH_2)-COOK]$ show powder SHG efficiencies 0.4, 1.0 and 0.3 times than that of m-nitroaniline (m-NA) respectively.

5 THIRD-ORDER NONLINEAR OPTICS IN ORGANOMETALLIC COMPOUNDS

Third-order NLO effects occur in extended π-conjugated systems. In 1973, Hermann *et al.*[125] reported that third-order susceptibility $\chi^{(3)}$ increases with the number of atoms in long-chain molecules. For example, *trans-β*-carotene, having eleven conjugated double bonds, exhibits a $\chi^{(3)}$ of the order of 10^{-12} esu. Theoretical calculations performed by Rustagi and Ducuing[126] and Agrawal *et al.*[127] concluded that $\chi^{(3)}$ should
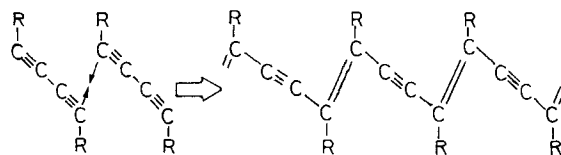
Figure 13 Solid-state polymerization of diacetylenes.

increase as the sixth power of the π-electron conjugation length. Flytzanis[128] also suggested that long π-electron conjugated structures are well suited for large $\chi^{(3)}$. In fact, π-electron delocalization has been assumed to be the source of large $\chi^{(3)}$ in conjugated molecules. Actually, inorganic semiconductors display very large $\chi^{(3)}$ (e.g. ZnS has a $\chi^{(3)}$ value of 10^{-5} esu), but their time response is slow. In 1976, Sauteret *et al.*[20] discovered a large $\chi^{(3)}$ value (8.5×10^{-10} esu), an ultra-fast time response (10^{-12} s) and a high damage threshold (10 GW cm^{-2}) in polydiacetylene-p-toluenesulphonate (PDA-PTS). Following this, the discovery of π-electron delocalized conducting polymers in the 1980s initiated further interest in third-order NLO properties. As a matter of fact, polydiacetylenes are still the most extensively studied polymeric systems.
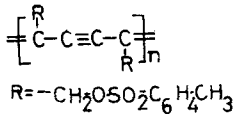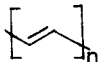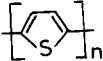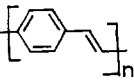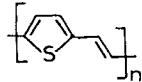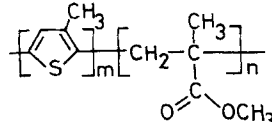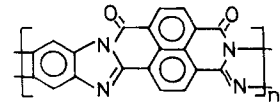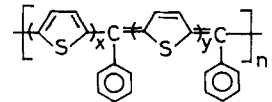
The one-dimensional conjugated π-electron backbone of the PDAs can be expressed as (R—C—C≡C—C—R)$_n$, where R represents substitutional side groups. The uniqueness of PDAs lies in the delocalized π-electron backbone responsible for the origin of NLO properties, and also in the wide variety of substitutional side groups which enable easy structural control and hence facilitate materials processing. Diacetylene molecules are highly reactive; therefore, a topochemical solid-state polymerization easily leads to the formation of polydiacetylenes[129, 130] as shown in Fig. 13.

There are many kinds of PDAs because of the variety of substitutional side groups. If R is $(CH_2)_mOCONHCH_2COO(CH_2)_3CH_3$ [referred to as m-butoxycarbonylmethylurethane (BCMU) polydiacetylenes], in the case where m equals to 3 or 4 these compounds are then abbreviated to P-3BCMU and P-4BCMU respectively. PDAs can be obtained in the form of ultrathin films, solutions or single crystals. The alignment of PDAs depends strongly on the chemical structure of the side groups. For example, planar structure of PDAs can be obtained for BCMU polymers that have a urethane group (—OCONH—) because of the formation of hydrogen bonding between the adjacent side groups.

The magnitude of $\chi^{(3)}$ values in PDAs is influenced by the side groups as well as by the fabrication techniques. For example, vacuum-deposited PDA films having side groups R = —(CH$_2$)$_4$OCONH(CH$_2$)$_2$CH$_3$ and —(CH$_2$)$_3$OH exhibit $\chi^{(3)}$ values of 3.80×10^{-10} and 1.10×10^{-11} esu respectively.[131, 132] Hsu et al.[133] reported $\chi^{(3)}$ values of $(1.0 \pm 0.07) \times 10^{-10}$ and $(2.0 \pm 0.2) \times 10^{-11}$ esu at $1.319 \mu m$ for single-crystalline and spin-coated amorphous 4-butoxycarbonylmethyl-urethane (4-BCMU) polydiacetylene (red form) thin films respectively; presumably the orientation of the polymer chains contributes to the large $\chi^{(3)}$ values of the crystalline films. A number of conjugated polymers have $\chi^{(3)}$ values comparable with that of PDAs (Table 5) and new conjugate organic polymeric systems are still emerging. Recently, Jenekhe et al.[140] reported even higher $\chi^{(3)}$ values for polythiophene superlattices. In a copolymeric system studied by the author (HSN),[138] although the incorporation of nonconjugated methyl methacrylate (MMA) blocks in the poly(3-methylthiophene) system leads toward transparency, on the other hand it restrains NLO $\chi^{(3)}$ responses. The present status of conjugated $\chi^{(3)}$ polymers is far short of realization in NLO

Table 5 Third-order nonlinear optical susceptibility $\chi^{(3)}$ of conjugated polymers

Polymer	Structure	$\chi^{(3)}$ (10^{-10} esu)	Wavelength (μm)	Measurement technique	Ref.
Polydiacetylene p-toluenesulphonate	R=—CH$_2$OSO$_2$C$_6$H$_4$CH$_3$	8.5	1.89	THG	20
Polyacetylene		80.0	1.064	THG	134
Polythiophene		0.30	1.06	DFWM	135
Poly(p-phenylene vinylene)		0.078	1.85	THG	136
Poly(thienyl vinylene)		0.32	1.85	TGH	137
P(3-MeTH/MMA)[a]		0.07	0.602	DFWM	138
BBL[a]		0.15 20.0	1.064 0.532	DFWM	139
PBTBQ[b]		2700.0	0.532	DFWM	140

[a]P(3-MeTH/MMA) = Poly(3-methylthiophene–methyl methacrylate)
[b]BBL = Poly{(7-oxo-7,10H-benz[d,e]imidazo[4',5':5, 6]benzimidazo[2,1-a]isoquinoline-3,4:10, 11-tetrayl)-10-carbonyl}
PBTBQ = Poly(α-[5,5'-bithiophenediyl]benzylidene-block-α-[5,5'-bithiophenequinodimethanediyl])
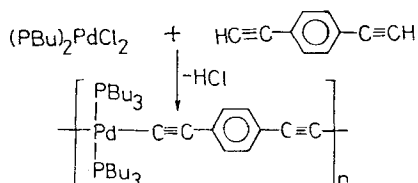
Figure 14 Formation of metal–polyyne complexes by poly-condensation.

devices, and hence new materials with large $\chi^{(3)}$ and other improved physico-chemical properties are still very much in demand.

5.1 Poly(metal-ynes)

Metal–polyyne polymers containing palladium metal in the conjugated acetylenic backbones have been prepared by Takahashi et al.[141] by polycondensation reactions in amines using cuprous iodide as catalyst (Fig. 14). The yellow polymer (Fig. 14) is highly soluble in benzene, toluene, tetrahydrofuran and methylene chloride because of the presence of bulky substituents on phosphorus which tend to reduce interactions between polymer molecules. This organometallic palladium–polyyne polymer is air-stable at room temperature and shows a decomposition point at $\sim$145 °C.[141]

Frazier et al.[142] investigated the third-order sus-ceptibility of palladium–polyyne by third-harmonic generation and powder limiting tech-niques. A 120 μm palladium–polyyne–polyimide cast film exhibits a nonlinear refractive index as much as 58 times higher than that of a carbon disulphide (CS$_2$) reference sample. The film shows a laser damage threshold of 33 GW cm^{-2}. Frazier et al.[143] also developed a relationship between the molecular structure of the metal–polyyne and its third-order molecular hyper-polarizability using a degenerate four-wave mix-ing (DFWM) technique. A platinum polyyne $-\!\left(Pt(PBu_3)_2\!-\!C\!\equiv\!C\!-\!C_6H_4\!-\!C\!\equiv\!C\right)\!_n$ exhibits a hyperpolarizability of 890×10^{-36} esu, more than two-fold larger compared with palladium polyyne (390×10^{-36} esu). Table 6 lists the γ-values of a series of metal polyynes:[142-144] these exhibit larger hyperpolarizabilities than the well-known organic NLO materials (p-nitroaniline, 2-methyl-4-nitroaniline and trans-stilbene).

5.2 Metallophthalocyanines

Metallophthalocyanines (MPc) (Fig. 15) are multipurpose materials applicable in biomedical engineering as well as in solid-state

technology.[145-149] The uniqueness of MPcs lies in their versatility, architectural flexibility and exceptional environmental stability. The phthalo-cyanine molecule has a two-dimensional π-electron conjugated system, and a number of modifications can be made either in the macro-cycle by incorporating a wide variety of central metal atoms or by substituting side groups at the peripheral sites of the macrocycle. As many as 60–70 different metal atoms can be embodied into the phthalocyanine macrocycle. This facili-tates in tailoring electrophysical parameters of MPcs over a very broad range. In addition to the extensively delocalized π-electron systems needed for third-order NLO responses, MPcs offer many other benefits.

The third-order nonlinear optical properties of a number of MPcs have been investigated in recent years. Ho et al.[150] reported third-harmonic generation (THG) in thin polycrystalline films of chlorogallium phthalocyanines (GaPc-Cl) and fluoroaluminium phthalocyanines (AlPc-F). The halogens (F and Cl) are attached to the central metal atom of the Pc macrocycle. A 1.2 μm thick film of GaPc-Cl exhibits a $\chi^{(3)}$ value of $\sim$2.5 × 10^{-11} esu, whereas a 0.8 μm thick film of AlPc-F shows a $\chi^{(3)}$ value of $\sim$5 × 10^{-11} esu, at 1.064 μm. GaPc-Cl has a mixed conformation of cofacially stacked (triclinic) and slipstacked (monoclinic) crystallites in a 1:1 ratio,[151] whilst, on the other

Table 6 Chemical structures and third-order hyperpolariza-bility of palladium polyyne and platinum polyynes (after Refs 142–144)

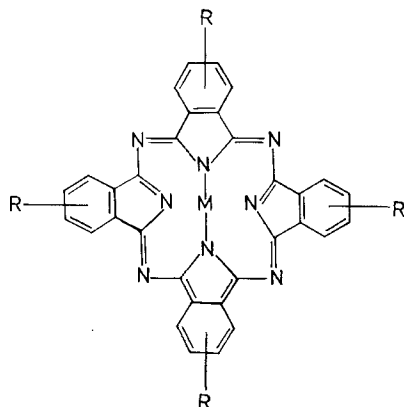| Polymer	Hyperpolarizability (γ) (10^{-36} esu)
	390
	102
	56
	856
	181

Figure 15 Chemical structures of metallophthalocyanines. In the case of Ga, Al, In, V and Ti, the central metal atom (M) contains substituents such as Cl, F and O, and SiPc contains the (OSiMePhOH)$_2$ group. The substituents on the benzene rings are either tetrakis(cumylphenoxy) groups or tetra-n-alkylthio groups (see Refs 145–149).

hand, AlPc-F possesses dominantly cofacially stacked crystallites;[152] therefore, the difference in $\chi^{(3)}$ results from the different crystal structures. Wada et al.[153] reported the THG of alkoxy derivatives of vanadyl phthalocyanine (VOPc). In this case, the alkoxy (R = OC$_2$H$_{2n+1}$) groups are substituted at the peripheral sites of VOPc. The VPOc thin film exhibits a $\chi^{(3)}$ value of 1.85 × 10^{-10} esu at a wavelength of 1.907 μm. The $\chi^{(3)}$ of VOPc is about two orders of magnitude larger than that of a metal-free phthalocyanine (H$_2$Pc). The trend of $\chi^{(3)}$ has been suggested in the order M = VO, Sn ≫ H$_2$, Ni, Co. A tetrakis (n-pentoxy) phthalocyanine [Pc(R$_4$)H$_2$], where R is OC$_5$H$_{11}$ and M is H$_2$ dispersed in poly(methyl methacrylate) (PMMA), shows $\chi^{(3)}$ values of 10^{-13} esu at 1.907 μm when dissolved in a weight ratio of 20:80 of [Pc(R$_4$)H$_2$] to PMMA.[153] The $\chi^{(3)}$ of metal-free tetrakis (cumylphenoxy) phthalocyanines and the corresponding platinum and lead complexes measured by degenerate four-wave mixing techniques has also been reported by Shirke et al.[154] The $\chi^{(3)}$ values of these Pcs is increased considerably by substitution of the central metal atom and, in particular, platinum is the most effective metal. Platinum and lead-containing phthalocyanines exhibit $\chi^{(3)}$ values of ~2 × 10^{-10} and ~2 × 10^{-11} esu at 1.064 μm respectively. PtPc has $\chi^{(3)}$ about an order of magnitude higher than that of PbPc and about 45 times larger than that of a metal-free (4 × 10^{-12} esu) form. Degenerate four-wave mixing studies of metal-free and silicon phthalocyanine (SiPc) have been

reported by Casstevens et al.[155] In the case of SiPc, two —OSiMeC$_6$H$_4$OH groups are attached to the silicon central metal atom of the Pc macrocycle. Langmuir–Blodgett films of [SiPc(OSiMeC$_6$H$_4$OH)$_2$] exhibit a $\chi^{(3)}$ value of ~1.8 × 10^{-9} esu at 0.602 μm.

Matsuda et al.[156] reported the third-order optical nonlinearities of CoPc, NiPc, CuPc, PtPc, Cl-InPc, Cl-AlPc, TiOPc and tetra-alkylthio-substituted (SC$_n$H$_{2n+1}$, where n is 4, 6, 7, 8, 10 and 12) CuPc and vanadium-oxo (vanadyl, VOPc) phthalocyanines. The non-substituted MPCs exhibit $\chi^{(3)}$ values in the range 10^{-11}–10^{-13} esu. A chloroindium phthalocyanine (Cl-InPc) showed the largest $\chi^{(3)}$ value of 1.30 × 10^{-10} esu at 1.907 μm. MPC derivatives possessing an axial ligand (i.e. Cl-AlPc, Cl-InPc, TiOPc, VOPc) show $\chi^{(3)}$ values more than an order of magnitude larger than those MPCs having no axial ligands. The $\chi^{(3)}$ values of vacuum-deposited MPc thin films are listed in Table 6. On the other hand, CuPc and VOPc having terminal tetra-alkyl thio substituents are solution-processable and their spin-coated thin films show $\chi^{(3)}$ values of the order of 10^{-11} esu. A 0.26 μm thick film of tetra-n-octylthiophthalocyanine copper exhibited $\chi^{(3)}$ values of 23 × 10^{-12} esu and 50 × 10^{-12} esu at 1.9 and 2.1 μm respectively. A 0.20 μm thick film of tetra-n-octylthiophthalocyanine vanadyl [(VOPc(C$_8$H$_{17}$S)$_4$] show the largest $\chi^{(3)}$ values of 4.1 × 10^{-12}, 18 × 10^{-12} and 31 × 10^{-12} esu at 1.5, 1.9 and 2.1 μm respectively. The THG measurements performed at three different wavelengths demonstrated that the $\chi^{(3)}$ values change as a function of measurement wavelengths and alkyl-thio chain length. Substitution of the long tetra-alkylthio chain decreases the magnitude of the $\chi^{(3)}$ value due to the dilution of the π-electron system. Also, long alkyl chains substituted at the peripheral sites of the MPc ring cause steric hindrance which prevents the cofacial stacking of Pc rings, and as a result large $\chi^{(3)}$ values displayed by these MPcs appear from the loose aggregation of molecules. This loose split packing, facilitated by unsymmetrical substitution, leads to large $\chi^{(3)}$ values.

Kajita et al.[157] measured the $\chi^{(3)}$ values of α- and β-forms of CuPc and of a copper naphthalocyanine (CuNPc). Both α- and β-phase CuPc show $\chi^{(3)}$ values of the order of 1.0 × 10^{-12} esu, whilst CuNPc exhibits a $\chi^{(3)}$ value of 3 × 10^{-12} esu at 1.064 μm. Chollet et al.[114] reported $\chi^{(3)}$ values of 4 × 10^{-12} and 3.4 × 10^{-12} esu for 78 and 62 nm thick CuPc films at 1.064 μm. The $\chi^{(3)}$ value of a

162 nm thick CuPc film at 1.907 μm corresponds to 2.1×10^{-12} esu, revealing thickness dependence of $\chi^{(3)}$ values.

Perry et al.[158] reported the optical nonlinearity of silicon naphthalocyanine having axial ligands, i.e. SiNPc[OSi(hexyl)$_3$]$_2$, of 4.0×10^{-12} esu for a solution concentration of 6×10^{-4} mol dm^{-3} in toluene using the 'Z-scan' technique. The SiNPc derivative has an excited-state absorption cross-section of 5×10^{-17} cm^2.

Lindle et al.[159] measured the third-order nonlinear susceptibilities of metal-free phthalocyanine (H$_2$Pc) and NiPc, CuPc, ZnPc, PdPc, and PtPc. The $\chi^{(3)}$ values of MPcs are affected by the nature of the central metal atom and by peripheral substitution. PdPc shows the largest $\chi^{(3)}$, of 2.0×10^{-10} esu. The $\chi^{(3)}$ values of MPcs are 2 to 45 times larger than that of H$_2$Pc. Lindle et al.[159] also made systematic studies of third-order optical nonlinearities of metallobisphthalocyanines to examine the interaction of two Pc macrocycles in charge-transfer transitions.

Third-order optical susceptibility studies of bisphthalocyanines of neodymium (NdPc$_2$), gadolinium (GdPc$_2$), lutetium (LuPc$_2$), yttrium (YPc$_2$), ytterbium (YbPc$_2$), europium (EuPc$_2$) and scandium (ScPc$_2$) and their anions indicate that the charge-transfer band does contribute to NLO properties of MPc$_2$. ScPc$_2$ shows a $\chi^{(3)}$ value as high as 1.70×10^{-9} esu. The nonlinear optical response of mono- and bis-phthalocyanines is faster than that of the optical pulsewidth of 35 ps. The third-order NLO properties measured at 1.064 μm using degenerate four-wave mixing (DFWM) techniques demonstrate that MPcs show large non-resonant $\chi^{(3)}$ values. Table 7 lists the third-order optical nonlinearities of a wide variety of unsubstituted, peripherally substituted and axially substituted MPcs; their $\chi^{(3)}$ values ranged from 10^{-9} to 10^{-13} esu depending on the material, measurement wavelength and techniques. Figure 15 shows the chemical structures of metallophthalocyanines which have been investigated with reference to nonlinear optics.

Table 7 Third-order nonlinear optical susceptibility $\chi^{(3)}$ of metallophthalocyanines (M-Pc)

Material M-Pc[a]	$\chi^{(3)}$ (10^{-12} esu)	Measurement wavelength (μm)	Measurement technique	Ref.
Cl-GaPc	25.0	1.064	THG	150
F-AlPc	50.0	1.064	THG	150
Cl-AlPc	15.0	1.907	THG	156
Cl-InPc	130.0	1.907	THG	156
VOPc	18.5	1.907	THG	153
TiOPc	27.0	1.907	THG	156
H$_2$PcCP$_4$	4.0	1.064	DFWM	154
PbPcCP$_4$	20.0	1.064	DFWM	154
PtPcCP$_4$	200.0	1.064	DFWM	154
R-SiPc	1800.0	0.602	DFWM	155
CoPc	0.76	1.907	THG	156
NiPc	0.80	1.907	THG	156
CuPc	4.0	1.064	THG	114
α-CuPc	1.0	1.064	THG	157
β-CuPc	1.0	1.064	THG	157
CuNPc	3.0	1.064	THG	157
(C$_4$H$_9$S)$_4$CuPc	3.7	1.907	THG	156
(C$_8$H$_{17}$S)$_4$CuPc	50.0	2.1	THG	156
(C$_{10}$H$_{21}$S)$_4$CuPc	26.0	1.907	THG	156
(C$_6$H$_{13}$S)$_4$VOPc	9.8	1.907	THG	156
(C$_8$H$_{17}$S)$_4$VOPc	31.0	2.1	THG	156
PtPc	200.0	1.064	DFWM	159
Sc(Pc)$_2$	1700.0	1.064	DFWM	159

[a]Abbreviations: CP$_4$ = Tetrakis(cumylphenoxy); R = (OSiMePhOH)$_2$; CuNPc = copper naphthalocyanine; Sc(Pc)$_2$ = scandium bisphthalocyanine.

Phthalocyanines show two characteristic absorption bands in the near-UV (Soret band at 300–400 nm) and in the visible (Q band at 600–800 nm) arising from the electronic transitions to π–π^* states of E_u symmetry.[145-147] In particular, the Q band is significantly affected by the environment of the phthalocyanine macrocycle. In fact, the characteristics of the Q band changes remarkably in the condensed state depending upon the nature of the central metal atom.[153] Now, analysis of $\chi^{(3)}$ data suggests that the large $\chi^{(3)}$ of [SiPc(OSiMePhOH)$_2$] arises due to the strong absorption at the measuring wavelength to (0.602 μm); hence $\chi^{(3)}$ is resonantly enhanced.[155] The $\chi^{(3)}$ values of GaPc-Cl, AlPc-F and PbPc are in the same range, whilst that of PtPc is one order of magnitude higher at the same measuring wavelength of 1.064 μm.[150, 154] The $\chi^{(3)}$ value of VOPc (1.85 × 10^{-10} esu) at 1.907 μm is in the same range as that of Pt-Pc (2.0 × 10^{-10} esu).[153] At the 1.064 μm wavelength, third-harmonic light is absorbed strongly at the Soret band; however, at 1.907 μm, the possibility of the absorption of third-harmonic light cannot be completely omitted.[153] Therefore, a large difference observed in $\chi^{(3)}$ values of MPcs results from the dispersion of $\chi^{(3)}$ in resonant and nonresonant regions as well as from different optical processes of THG and DFWM techniques.

Nonlinear optical properties of phthalocyanines are also influenced by film preparation methods. Kalbeitzel et al.[160] reported that the relaxation time changes from nanoseconds to picoseconds depending on film preparation. Chollet et al.[114] demonstrated the thickness dependence of $\chi^{(3)}$ for CuPc films.

5.3 Metallocenes

Ferrocene derivatives have been considered important for both second- and third-order NLO effects. Winter et al.[161] measured the molecular hyperpolarizability of ferrocene in the melt, in solution and for a liquid derivative, bis(trimethylsilyl) ferrocene. The third-order coefficient of ferrocene is three times larger than that of nitrobenzene. The nonlinear refractive indices n_2 of ferrocene (solution), ruthenocene, hafnocene, zirconocene and bis(trimethylsilyl)ferrocene (BTMSF), measured by the optical power limiter technique, correspond to 2.6 × 10$^{=13}$, 3.3 × 10^{-11},
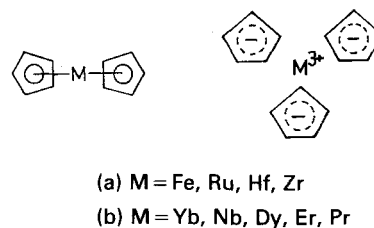

(a) M = Fe, Ru, Hf, Zr
(b) M = Yb, Nb, Dy, Er, Pr

Figure 16 Structures of (a) ferrocene (Fe), ruthenocene (Ru), hafnocene (Hf) and zirconocene (Zr), and (b) rare-earth compounds M(C$_5$H$_5$)$_3$.

1.3 × 10^{-11}, 1.0 × 10^{-11} and 1.51 × 10^{-11} esu respectively. The ratio of n_2 for linear and circular polarized light (n_2—linear)/n_2—circular) for ruthenocene and BTMSF is 0.6 and 0.7 respectively.[161] The metallocenes seem interesting since many metal atoms can be incorporated as well as substitution being possible on the ring.

Recently, aryl and vinyl derivatives of ferrocene have been synthesized by Ghosal et al.[162] The molecular polarizability of these ferrocene derivatives increases with increase of the conjugated π-electron system, but hyperpolarizability values are much smaller than that reported by Winter et al.[161] Oliver et al.[163] also reported the third-order optical nonlinearities of the tricyclopentadienyl-ides of Yb, Nd, Er, Dy and Pr which have $\chi^{(3)}$ values of 9.3 × 10^{-13}, 3.07 × 10^{-13}, 7.16 × 10^{-14}, 1.36 × 10^{-13} and 7.16 × 10^{-14} esu respectively (Fig. 16).

5.4 Polysilanes and polygermane

Although polysilanes are sometimes not regarded as true organometallics since silicon is a metalloidal element, they do have interesting nonlinear optical properties (similar to polygermane derivatives) and these will be discussed here. In organosilane polymers, the monomer unit consists of a central silicon atom which is bonded with two organic substituent groups. In a linear polysilane backbone, all monomeric units are linked together via silicon atoms. Since polysilanes possess only silicon atoms in the polymer backbone (Fig. 17), Si–Si σ-electron delocalization leads to
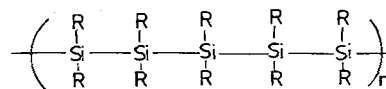

Figure 17 Chemical structure of polysilanes.

interesting properties. A wide variety of polysilanes can be obtained by varying substituted side groups. These σ-bonded backbone of polysilanes offers several advantages from practical viewpoints:[164, 165]
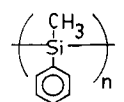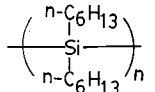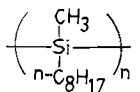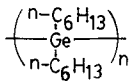
(i) Polysilanes are transparent materials at all visible wavelengths.

(ii) Polysilanes are processable materials, and good-quality thin films can be fabricated either by solvent casting or by melt processing.

(iii) Polysilanes show high thermal stability (between 250 and 300 °C) and their glass transition temperature (T_g) ranges from -75 to 120 °C.

(iv) Polysilanes exhibit good environmental stability.

In regard to third-order nonlinear optics, polysilanes are polarizable materials whose electronic properties closely resemble conjugated π-electron systems such as poly(diacetylenes), polyacetylenes, polythiophenes, etc. (Table 5). The first report on nonlinear optical properties of polysilanes appeared in 1986. Kajzar et al.[166] measured a $\chi^{(3)}$ value of 1.50×10^{-12} esu at 1.064 μm for poly(methylphenylsilane) (PMPS). Yang et al.[167] reported a $\chi^{(3)}$ value of 2.0×10^{-12} esu using a picosecond optical Kerr gate, and a $\chi^{(3)}$ value of 1.6×10^{-12} esu by the DFWM technique. The

third-order nonlinear optical response is found to be faster than 3 ps arising from an electronic contribution in PMPS. Baumert et al.[168] reported $\chi^{(3)}$ studies of PMPS as a function of temperature, film thickness and wavelength. Although PMPS shows no detectable changes in $\chi^{(3)}$ with temperature, its $\chi^{(3)}$ value changes remarkably with film thickness. The $\chi^{(3)}$ value of PMPS increases from 1.9×10^{-12} to 4.2×10^{-12} esu at 1.907 μm as the film thickness changes from 1200 nm to 120 nm respectively. A 120 nm thick PMPS film shows $\chi^{(3)}$ as high as 7.2×10^{-12} esu at 1.064 μm.

Baumert et al.[168] also investigated $\chi^{(3)}$ for poly(di-n-hexylsilane) (PDHS) and poly(di-n-hexylgermane) (PDHG) using the THG method. Temperature-, thickness- and wavelength-dependent studies show very interesting NLO features. The thinnest PDHS film (50 nm thickness) shows the largest $\chi^{(3)}$ value of 11.3×10^{-12} esu at 1.064 μm. Similar characteristics are also observed for PDHG. A 295 nm thick PDHG film shows $\chi^{(3)}$ values of 3.3×10^{-12} and 1.1×10^{-12} esu at 1.064 and 1.907 μm respectively. The $\chi^{(3)}$ values of PDHS and PDHG change significantly with variation of polymer backbone conformational structures induced by thermal treatments. McGraw et al.[169] reported a $\chi^{(3)}$ value of 2.9×10^{-12} esu for poly(n-octylmethylsilane) (POMS) at 0.532 μm. Table 8 lists the chemical structures, $\chi^{(3)}$ values and measurement techniques for PMPS, PDHS, PDGH and POMS for

Table 8 Third-order nonlinear optical susceptibility $\chi^{(3)}$ of polysilanes and polygermanes

Polymer	Chemical structure	$\chi^{(3)}$ (10^{-12} esu)	Measurement wavelength (μm)	Technique	Absorption maximum (nm)	Ref.
Poly(phenylmethylsilane)		1.5	1.064	THG	341	166
		7.2	1.064	THG		168
		4.2	1.907	THG		168
Poly(di-n-hexylsilane)		11.3	1.064	THG	317	168
		1.3	1.907	THG		
Poly(n-octylmethylsilane)		2.9	0.532	THG	309	169
Poly(di-n-hexylgermane)		6.5	1.064	THG	320	168
		1.4	1.907	THG		
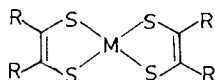
(M = Ni, Pt; R = H, CH$_3$, CF$_3$, CN, C$_6$H$_5$ etc.)

Figure 18 Chemical structure of metal dithiolenes.

comparison. Optical transparency and large non-resonant third-order optical nonlinearities demonstrate the superiority of polysilanes over conjugated π-electron polymers.

5.5 Miscellaneous organometallics

Oliver et al.[163] investigated third-order optical nonlinearities of metal dithiolenes (Fig. 18). Metal dithiolenes show a strong near-infrared absorption band, which can be adjusted from 700 to 1400 nm by substituting appropriate functional groups. The methyl- and phenyl-substituted nickel dithiolenes show nanosecond n_2 values of 2.7×10^{-10} and 8.9×10^{-11} esu respectively. The nickel complexes in which the ligand sulphur atoms are replaced by selenium and the substituents are CF$_3$ show a $\chi^{(3)}$ value of 1.4×10^{-13} esu. A platinum dithiolene complex (where the central metal ion is platinum) having cyano (CN) substituents exhibits $\chi^{(3)}$ value of 4.2×10^{-12} esu. The $\chi^{(3)}$ values of metal dithiolene complexes are affected both by the central metal atom as well as by the substituents (R). A nickel dithiolene complex containing phenyl substituents exhibits a $\chi^{(3)}$ value as large as 3.67×10^{-11} esu. A bis[1,2-ethenedithiolato(2−)-S,S']platinum tetrabutyl-ammonium shows a $\chi^{(3)}$ value of about 7.16×10^{-14} esu. Since these metal dithiolenes absorb between 700 and 1400 nm, these $\chi^{(3)}$ values are resonantly enhanced. The $\chi^{(3)}$ values of metal dithiolenes range from 7.16×10^{-14} to 3.6×10^{-11} esu depending on the nature of the compounds.

Lindle et al.[159] measured the $\chi^{(3)}$ values of metal complexes of o-aminobenzenethiol (ABT) (Fig. 19). The $\chi^{(3)}$ value of ABT increases significantly by metal substitution and a nickel complex of ABT shows the largest $\chi^{(3)}$ of the order of 2.0×10^{-9} esu, and γ value of 2×10^{-31} esu.
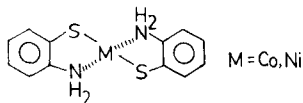

Figure 19 Chemical structure of metal complexes of ABT (after Ref. 159).

Funatsu et al.[170] reported the third-order non-linear susceptibilities of halogen-bridged mixed-valence platinum complexes of general formula [Pt(en)$_2$][Pt(en)$_2$X$_2$](ClO$_4$)$_4$, where X = Cl, Br or I and en = ethylenediamine. These linear-chain complexes have a one-dimensional electron system along the chain axis and possess inversion centres. The Pt–Cl complex exhibits $\chi^{(3)}$ values of 1.2×10^{-12} and 4.1×10^{-12} esu at 1.907 and 1.064 μm respectively. The Pt–Br complex has $\chi^{(3)}$ values of 1.7×10^{-11} esu at 1.907 μm and 7.0×10^{-11} esu at 1.064 μm. Wada and Yamashita[171] calculated the $\chi^{(3)}_{zzzz}$ of these complexes employing a three-level model considering the ground state and odd and even charge-transfer excitons. The Pt–Cl, Pt–Br and Pt–I complexes have $\chi^{(3)}$ values in the range 10^{-12}–10^{-8} esu. These nonresonant values increase in the order Cl < Br < I due to increase of the oscillator strengths and to decrease of the resonant energies.

6 POSSIBLE APPLICATIONS

Applications of nonlinear optical (NLO) materials have been realized in opto-electronic technology. Since there exists a wide variety of NLO processes, their numerous related NLO applications could be considered: these include harmonic generators, electro-optic modulators, parametric amplifiers, optical bistabilizers, frequency up-and-down converters, high-speed optical gates, phase conjugation, image processing, all-optical signal processing, etc.[172-176]

A simple example of an application of NLO materials is to change the frequency of laser light via generation of second and third harmonics. For simplicity, SHG materials can convert a 1064 nm Nd–YAG laser beam into a 532 nm green laser beam, while on the other hand THG materials can convert the same 1064 nm near-infrared laser beam into a 355 nm ultraviolet laser beam; hence NLO materials can be used as frequency doublers and frequency triplers respectively.

Many inorganic as well as organic NLO materials especially suited to these applications are being developed. Here the discussion is limited to the promise of organometallic materials and, so far, only a few reports have appeared in this connection.

Recently, Garito and Wu[177] reported for the first time absorptive optical bistability in a randomly glassy ultrathin film consisting of quasi-
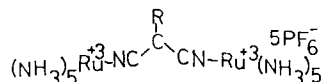
Figure 20 Transition-metal-based dye molecule; R = H or tert-butyl.

two-dimensional conjugated discs of silicon naphthalocyanine oligomer (SINC). SINC contains the —(OSiMeO(CH$_2$)$_3$NHCO(CH$_2$)$_6$-CONH(CH$_2$)$_3$(OH$_2$) group attached to the silicon central metal atom of the naphthalocyanine macrocycle. High optical quality thin films of SINC and its poly(methyl methacrylate) (PMMA) alloy can be formed by a spin-coating technique. The SINC films exhibits a nonlinear refractive index (n_2) of 1×10^{-4} cm^2 kw^{-1} at 810 nm, comparable with that of gallium arsenide (GaAs).[178] This n_2 value has been claimed to be the largest observed to date for a conjugated organic structure. This is also the first case of electronic absorptive optical bistability on a nanosecond time scale in a nonlinear Fasbry–Perot interferometer using a saturably absorbing SINC film as the nonlinear optical medium.

Nonlinear optical waveguides of a transition-metal-based dye molecule have been reported by Cahill.[179] Two pentamine malonitrile ruthenium dyes (Fig. 20) show strong ligand-to-metal charge-transfer bands near 800 nm. A noncentrosymmetric waveguide for SHG is possible by controlling the refractive index and by adjusting the concentration of the organometallic dye molecules.

As discussed earlier, transparent polysilane films exhibit large non-resonant third-order optical nonlinearities. Schellenberg et al.[180, 181] reported the fabrication of a birefringent grating using a 700 nm thick film of poly(di-n-hexylsilane). The writable birefringence occurs by a process of chain scission caused by two-photon exposure. The two-photon excitation causes localized scission resulting in a permanent birefringence in polysilane films. This unique effect can be utilized in fabricating other nonliner optical devices.

The optical transparency of organosilicon compounds suggests their great potential in nonlinear optical devices. In fact, a majority of organometallics exhibit strong colour; hence, particularly for SHG devices, tailoring of transparency is an important factor, whilst on the other hand coloured organometallics should have potential applications in third-order nonlinear optical

devices. Therefore, applications of organometallics should be judged on the basis of their optical transparency and also by reference to the magnitude of the second- and third-order nonlinear optical susceptibilities.

Zyss[182] classified organic NLO materials into three categories: (1) coloured, (2) yellow, and (3) transparent materials, and suggested their possible application with respect to their solid-state transparency cut-off. The coloured materials refer to those of red, blue and dark-coloured materials showing cut-off wavelength above the 550 nm region. These materials are conjugated systems such as stilbene derivatives, diazo molecules, 'push–pull' polyenes, etc. The yellow-coloured materials show cut-off wavelengths in the 500 nm region and include p-nitroaniline derivatives such as 2-methyl-4-nitroaniline (MNA), N-(4-nitrophenyl)-L-prolinol (NPP), 3-methyl-4-nitropyridine-1-oxide (POM), 4-(N, N'-dimethylamino)-3-acetamidonitrobenzene (DAN), methyl (2,4-dinitrophenyl)aminopropanoate (MAP), 3-methyl-4-methoxy-4'-nitrostilbene (MMONS), etc. These yellow materials seem promising for electro-optic modulation or switching of visible or near-infrared lasers. The transparent materials e.g. urea-like molecules, show cut-off wavelengths below the 450 nm region. The transparency region can be controlled to some extent by molecular engineering of the donor and acceptor functionalities. The specific applications of organic NLO materials are associated with the transparency/efficiency trade-off. Therefore, for molecular design of organometallic materials, these relationships should be considered. From the applications point of view, molecular engineering, the synthesis of new organometallics for efficient NLO properties, and transparency/efficiency trade-offs are of great importance.

7 CONCLUSION

During the past decades, there has been tremendous interest and also progress in developing new inorganic as well as organic materials for nonlinear optics. Nevertheless, nonlinear optical studies show that organometallic compounds are versatile materials which can be used, from single crystals to Langmuir–Blodgett films. The main reason for studying organometallics is the wide variation in NLO properties that can be attained by modification of the chemical structures. At

present, though organometallics are far from being truly explored as important materials for NLO devices, considerable progress is expected with the evolution of new materials. Probably, a finite-sized conjugate system either of conjugated cyclic structures containing a metal or organometallic complexes should be sufficient for obtaining the large third-order optical nonlinearities. In addition, electron-donor and/or electron-acceptor groups attached to the finite-sized conjugated structures can also play a major role. The demands for large NLO figures of merit, high resistance to laser damage, good environmental stability and overall high-performance materials will continue. In this respect, organometallic materials that have been molecularly engineered well are required. In addition, a better understanding of the NLO process is also equally important in order to achieve the ultimate goal of fabricating novel NLO devices. Although much research activity is going on in this field at present, the potential will increase if new materials become more readily available to the scientific community. In particular, chemists can provide tailor-made organic materials and can play a significant role in boosting novel research in this area. New materials originating from the laboratory offer a great opportunity in the development of new-generation NLO materials in collaborative efforts with materials scientists, physicists and optical engineers for profitable impact, on the new emerging opto-electronic technologies.

8 LATE ADDITIONS

8.1 Second-order nonlinear optics in organometallics (miscellaneous)

Pollagi et al.[183] investigated the optical second-harmonic generation of a new class of one-dimensional conjugated polymers of the type [N=M(OR)$_3$]$_n$, where M = Mo, W and R = CMe$_3$, CMe$_2$CF$_3$. These conjugated one-dimensional polymers have the structure shown in Fig. 21.
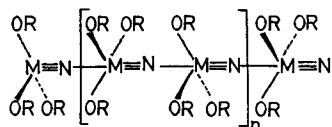
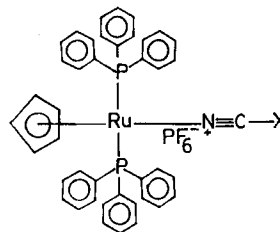**Figure 21** Structure of one-dimensional conjugated polymers [N = M(OR)$_3$]$_n$

Figure 22 Chemical structure of transition-metal complexes (after Ref. 184).

A [MoN(OCMe$_3$)$_3$]$_n$ polymer crystallizes in noncentrosymmetric space group $P6_3cm$ and displays SHG efficiency 0.25 times that of urea. A [WN(OCMe$_3$)$_3$]$_n$ polymer crystallizes in space group $P6_3$ and shows SHG efficiency 0.20 times that of urea. In contrast, a [MoN(OCMe$_2$Et)$_3$]$_n$ polymer shows no SHG activity, while a [MoN(OCMe$_2$CF$_3$)$_3$]$_n$ polymer shows SHG 0.35 times that of urea at 1.064 μm. The SHG activity and the emission energy of these polymers are sensitive to the nature of the alkoxide ligands as well to the effective conjugation chain length of the [MN]$_n$ backbone.

Richardson et al.[111,184] investigated the second-order optical nonlinearity of a series of novel transition-metal complexes. Figure 22 shows the chemical structures of organoruthenium complexes. Each organoruthenium complex consists of a common ruthenium-centred head-group with an entirely different conjugation region (X). The second-order hyperpolarizabilities measured by the electric-field induced second-harmonic generation (EFISH) technique at 1.064 μm show a significant effect of both conjugation length and type of conjugation. The β value of a biphenyl system (X = —C$_6$H$_4$—C$_6$H$_4$—OC$_{12}$H$_{25}$) is 20 × 10^{-30} esu, while that of a single phenyl ring having the same alkoxy group (X = —C$_6$H$_4$—OC$_{12}$H$_{25}$) is 3.5 × 10^{-30} esu. Probably, the β value of the *trans*-stilbene system (X = —C$_6$H$_4$—CH=CH—C$_6$H$_4$—OC$_{13}$H$_{27}$) is 37 × 10^{-30} esu and the β value of a carbon–carbon triple bond system (X = —C$_6$H$_4$—C≡C—C$_6$H$_4$—OC$_{13}$H$_{27}$) is 25 × 10^{-30} esu. In these organoruthenium complexes, the alkoxy chain acts as an electron donor while the nitrile (C≡N) group acts as an electron acceptor. These organoruthenium complexes form Langmuir–Blodgett films and a pentoxy group is sufficient to form good-quality Langmuir–Blodgett layers of the complexes.

Sakaguchi et al.[185,186] reported second-harmonic emission from ruthenium(II)–bipyridine complexes. The LB films of the RuC$_{18}$B ($n = 17$) (Fig.

23) complex exhibit strong second-harmonic light emission of 532 nm. The second-harmonic light intensity of the $RuC_{18}B$ complex decreases significantly by laser pulses of either 355 or 460 nm just before Nd–YAG laser illumination at 1.064 μm. The change of SH light intensity was examined by observing transient absorption after UV laser irradiation. The transient absorption spectrum in methanol solution shows two absorption bands: one at 380 nm due to the bipyridine anion radical and another at 500–900 nm due to Ru^{3+}, while the metal–ligand charge-transfer (MLCT) band of 480 nm disappears on excitation. This phenomenon demonstrates that the transfer of an electron takes place from Ru^{2+} to the bipyridine moiety upon UV laser excitation. The significant change in SH light intensity occurs because of the reduction of molecular hyperpolarizability on going from the ground state to a metal–ligand charge-transferred excited state, but not because of the change in refractive indices and phase-matching conditions.[186] This represents the first example of optical modulation based on SHG.

Recently, Matsuo et al.[187] investigated the effect of alkyl chain length [i.e. $(CH_2)_n$—CH_3 where n is 1, 5, 11, 15 and 17] on the SHG activity of ruthenium(II)–bipyridine complexes. The SHG intensity increases as the number of carbon atoms in the alkyl chain increases up to a hexadecyl chain (n = 15) and shows a decline for an octadecyl chain (n = 17). These complexes also exhibit a significant effect of the nature of the glass surface on which the films are deposited for SHG measurements. The hydrophobic surface obtained by treatment with a silane derivative shows that the SHG intensity changes from 4 to 80 on going from a hexyl chain (n = 5) to a hexadecyl chain (n = 15). Though similar effects on HCl and NaOH ionized glass surfaces were also observed, these treatments further increased the SHG intensity. The relative SHG intensity of ruthenium(II)-bipyridine complexes having a
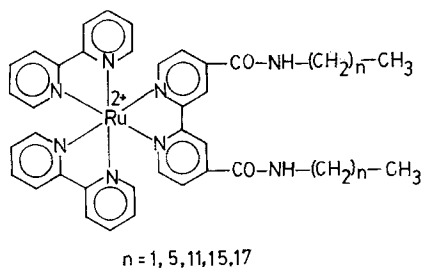

n = 1, 5, 11, 15, 17

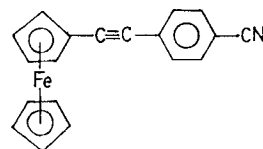Figure 23 Structure of ruthenium(II)–bipyridine complexes.

Figure 24 Ferrocenylphenylacetylene.

hexyl chain changes from 4 to 68 to 72 as the glass surface is treated with silane derivatives, HCl and NaOH respectively.

Perry et al.[188] reported the SHG activity of asymmetric end-capped acetylenic oligomers. The SHG efficiency of a ferrocenylphenylacetylene (Fig. 24) is 3.7 times that urea, at 1.907 μm. This SHG efficiency is about 15 times lower than an analogous ferrocene compound, cis-[1-ferrocenyl-2-(4-nitrophenyl)ethylene].[97] In this compound, the ferrocene group acts as electron donor, while CN acts as an acceptor.

8.2 Third-order nonlinear optics in organometallics (miscellaneous).

8.2.1 Porphyrin derivatives

Rao et al.[189] reported the third-order nonlinear optical susceptibility of several metallo- and metal-free tetrabenzporphyrin derivatives. The $\chi^{(3)}$ values were measured in tetrahydrofuran solution at 532 nm using a degenerate four-wave mixing (DFWM) technique. These tetrabenzporphyrins are substituted at their meso-positions with a variety of aryl and aliphatic functional groups. A zinc meso-tetra(p-dimethylaminophenyl)tetrabenzporphyrin shows the largest $\chi^{(3)}$ value of 2.8×10^{-8} esu. In addition, four other zinc derivatives containing tetramethyl, m-fluorophenyl, p-methoxyphenyl and p-methylphenyl functional groups at meso-positions have $\chi^{(3)}$ values of 1.5×10^{-8}, 1.3×10^{-8}, 1.4×10^{-8} and 1.2×10^{-8} esu respectively. A zinc hexadecafluorotetrabenzporphyrin (i.e., containing fluoro substituents at the benzo positions) exhibits a $\chi^{(3)}$ value of 2.0×10^{-9} esu. A magnesium octamethyltetrabenzporphyrin (i.e. having methyl groups at the benzo positions) shows $\chi^{(3)}$ of 8.0×10^{-9} esu. The $\chi^{(3)}$ values of both, a metal-free tetrabenzporphyrin and a zinc meso-tetraphenyltetrabenzporphyrin correspond to 3.0×10^{-9} esu. The $\chi^{(3)}$ values of these nine tetrabenzporphyrin having different functional groups are four to five orders of magnitude larger than that of the reference CS_2 sample. In particular, the tetrabenzporphyrin derivatives having stronger electron-donating groups on the meso-

positions show the larger $\chi^{(3)}$ values. The $\chi^{(3)}$ values of these compounds are the largest so far reported among metallophthalocyanine compounds (see Table 7). The zinc *meso*-tetra(*p*-dimethylaminophenyl)tetrabenzporphyrin compound which has the largest $\chi^{(3)}$ of 2.8×10^{-8} esu shows two absorption peaks at about 450 nm and 640 nm and transparency in the green region of the optical spectrum; therefore, the $\chi^{(3)}$ value may have the possibility of a resonant enhancement. The optical nonlinearity has predominantly an electronic origin with a response time faster than 15 ps.

Maloney *et al.*[190] investigated the third-order nonlinear optical properties of several tetraphenylporphyrin (TPP) compounds (Fig. 25). The $\chi^{(3)}$ values measured by the DFWM technique at 532 nm in toluene solution for a metal-free (H$_2$TPP), ZnTPP and CoTPP are about 2.86×10^{-11}, 1.43×10^{-11} and 7.16×10^{-12} esu respectively. The effective third-order nonlinear susceptibility values of H$_2$TPP, ZnTPP and CoTPP calculated taking into account the thermally induced refractive index changes are 2.07×10^{-11}, 2.0×10^{-11} and 1.21×10^{-11} esu respectively. The chemical modification caused by the metal substitution affects the optical nonlinearity. MgTPP has also been used as the nonlinear medium which enhances the phase conjugation reflectivity by ~300% at an optical delay of 0.7 ns.[191]

Sakaguchi *et al.*[192] reported the third-order optical nonlinearities of 5,10,15,20-tetrakis(4-pentadecylphenylporphyrins) containing metal atoms, i.e. Co, Ni, Zn, Cu and VO. These M-TPP compounds of 0.02–0.05% concentration in benzene solution show $\chi^{(3)}$ values in the region of ~10^{-11} esu. The $\chi^{(3)}$ shows concentration dependence. A Cu-TPP compound having 0.05% weight dissolved in benzene exhibits a $\chi^{(3)}$ value of 1.8×10^{-11} esu as determined by the DFWM technique.

8.2.2 Miscellaneous organometallics

Perry *et al.*[188] investigated the third-order nonlinear susceptibility of several symmetric end-

capped acetylenes. A bisferrocenyl compound, i.e. Fc—(C≡C)$_2$—Fc where Fc refers to the ferrocene moiety, shows a $\chi^{(3)}$ value of 2.25×10^{-12} esu at 1.907 μm as determined by the THG technique in toluene solution. The $\chi^{(3)}$ of the bisferrocenyl compound is more than twice that of a phenyl-substituted diacetylene, C$_6$H$_5$—(C≡C)$_2$—C$_6$H$_5$, at the same wavelength. The bisferrocenyl compound shows an absorption band at 438 nm: therefore the $\chi^{(3)}$ value may be affected by a three-photon pre-resonance process.

Shirk *et al.*[193] reported the third-order optical susceptibility of a series of transition metal tetrakis(cumylphenoxy)phthalocyanines (MPcCP$_4$) at 1.064 μm. In an earlier study[154] the $\chi^{(3)}$ values of H$_2$PcCP$_4$, PtPcCP$_4$ and PbPcCP$_4$ had been reported. The phthalocyanines substituted with the first row of transition metals (Co, Ni, Cu and Zn) and also the Ni, Pd and Pt triad are discussed here. CoPcCP$_4$, NiPcCP$_4$, CuPcCP$_4$, ZnPcCP$_4$, and PdPcCP$_4$ exhibit the $\chi^{(3)}$ values of 8×10^{-11}, 6×10^{-11}, 4×10^{-11}, 7×10^{-12} and 2×10^{-11} esu respectively.

Lindle *et al.*[194] investigated the third-order nonlinear susceptibilities of solutions of transition-metal complexes of benzenedithiol [C$_6$H$_5$—(SH)$_2$] using the DFWM technique at 1.064 μm. The transition-metal complexes of benzenedithiol and *o*-aminobenzenethiol are an interesting class of NLO materials.

The organometallic (BEDT-TTF)$_4$Re$_6$Se$_5$Cl$_9$ [where BEDT-TTF refers to bis(ethylenedithio)tetrathiofulvalene], which has single sheets of BEDT-TTF donor alternating with all-inorganic cluster ions, shows a $\chi^{(3)}$ of 1.6×10^{-8} esu,[195] almost similar to a cation radical salt of (BEDT-TTF)$_2$I$_3$ ($\chi^{(3)} = 5 \times 10^{-8}$ esu). A single crystal of (BEDT-TTF)$_8$SiW$_{12}$O$_{40}$ which has a sandwiched structure also exhibits a $\chi^{(3)}$ of the order of 10^{-8} esu. The large optical nonlinearity probably arises from the high delocalization of the donor planes.
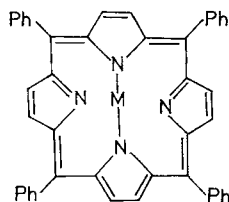

Figure 25 Structure of TPP compounds.

REFERENCES

1. Maiman, T H *Nature (London)*, 1960, 187: 493
2. Franken, P A, Hill, A E, Peters, C W and Weinreich, G *Phys. Rev. Lett.*, 1961, 7: 118
3. Kleinman, D A *Phys. Rev.*, 1962, 126: 1977
4. Giordmaine, J A *Phys. Rev. Lett.*, 1962, 8: 19
5. Maker, P D, Terhune, R W, Nisenoff, N and Savage, C M *Phys. Rev. Lett.*, 1962, 8: 21
6. Akhmanov, S A, Kovrigin, A I, Khoklov, R V and Chunaev, O N *Sov. Phys. JEPT*, 1964, 18: 919
7. Wang, C C and Racette, G W *Appl. Phys. Lett.*, 1965, 6: 169
8. Bjorkholm, J E *Phys. Rev.*, 1966, 142: 126
9. Bloembergen, N and Pershan, S *Phys. Rev.*, 1962, 128: 606
10. Giordmaine, J A and Miller, R C *Phys. Rev. Lett.*, 1965, 14: 973
11. Bloembergen, N *Nonlinear Optics*, Benjamin, New York, 1965
12. Kurtz, S K and Robinson, F N H *Appl. Phys. Lett.*, 1967, 10: 62
13. Jeggo, C R and Boyd, G D *J. Appl. Phys.*, 1970, 41: 741
14. Levine, B F *Phys. Rev. Lett.*, 1969, 22: 787
15. DiDomenico M, Jr *J. Appl. Phys.*, 1969, 40: 735
16. Chemla, D S, Oudar, J L and Jerphagnon, J *Phys. Rev. B*, 1975, 12: 4534
17. Davydov, B L, Derkacheva, L D, Dunina, V V, Zhabotinskii, M E, Zolin, V F, Koreneva, L G and Samokhina, M A *Sov. Phys. JEPT, Lett.*, 1970, 12: 16
18. Davydov, B L, Derkacheva, L D, Dunina, V V, Zhabotinskii, M E, Zolin, V F, Koreneva, L G and Samokhina, M A *Opt. Spectrosc.*, 1970, 30: 274
19. Davydov, B L, Dunina, V V, Zolin, V F and Koreneva, L G *Opt. Spectrosc.*, 1973, 34: 150
20. Sauteret, C, Hermann, J P, Frey, R, Pradere, F, Ducuing, J, Baughman, R H and Chance, R R *Phys. Rev. Lett.*, 1976, 36: 956
21. Byer, R L *Annl. Rev. Mater. Sci.*, 1974, 4: 147
22. Zernike, F and Midwinter, J *Applied Nonlinear Optics*, Wiley, New York, 1973
23. Flytzanis, C in *Quantum Electronics: A Treatise*, vol 1, Rabin, H and Tang, C L (eds) Academic, New York, 1975, p 19
24. Hanna, D C, Yuratich, M A and Cotter, D *Nonlinear Optics of Free Atoms and Molecules*, Sringer, Berlin, 1981
25. Oudar, J L and Chemla, D S *Opt. Commun.*, 1975, 13: 164
26. Levine, B F *Chem. Phys. Lett.*, 1976, 37: 516
27. Williams, D J *Angew. Chem. Int. Ed. Engl.*, 1984, 23: 690
28. Oudar, J L *J. Chem. Phys.*, 1977, 67: 446
29. Oudar, J L and Chemla, D S *J. Chem. Phys.*, 1977, 66: 2664
30. Kurtz, S K and Perry, T T *J. Appl. Phys.*, 1968, 39: 3798
31. Ashkin, A, Boyd, G D and Dziedzic, J M *Phys. Rev. Lett.*, 1963, 11: 14

32. Francois, G E and Siegman, A E *Phys. Rev. A*, 1965, 139: 4
33. Louisell, W H, Yariv, A and Siegman, A E *Phys. Rev.*, 1961, 126: 1646
34. Byer, R L and Harris, S E *Phys. Rev.*, 1968, 168: 1064
35. Fisher, R A *Optical Phase Conjugation*, Academic, New York, 1983
36. Burns, W K and Bloembergen, N *Phys. Rev. B*, 1971, 4: 3437
37. Soileau, M J, Williams, W E and Van Stryland, E W *IEEE J. Quantum Electron.*, 1983, QE-19: 731
38. Etemad, S and Baker, G L *Synth. Metals*, 1989, 28: D159
39. Baumgartener, R and Byer, R L *IEEE J. Quantum Electron.*, 1979, QE-15: 432
40. Zumsteg, F C, Bierlein, J D and Gier, T E *J. Appl. Phys.*, 1976, 47: 4980
41. Bierlein, J D and Vanherzeele, H *J. Opt. Soc. Am. B*, 1989, 6: 622
42. Hon, D In: *Laser Handbook*, vol. 3, Stitch, M L (ed), North-Holland, Amsterdam, 1979, p 421, and references therein
43. Chen, C T, Wu, Y, Jiang, A, Wu, B, You, W, Li, R and Lin, S *J. Opt. Soc. Am. B*, 1989, 6: 616
44. Chen, C T, Wu, B C, Jing, A D and You, G M *Sci. Sin. B*, 1985, 28: 235
45. Lu, S F, Ho, M Y and Huand, J L *Acta Phys. Sin.*, 1982, 31: 948 (in Chinese)
46. Glass, A M *Materials Research Socity (MRS) Bulletin*, August 1988, pp 16–29
47. Fan, Y X, Eckardt, R C, Byer, R L, Route, R K and Fiegelson, R S *Appl. Phys. Lett.*, 1984, 45: 313
48. Franken, P A and Ward, J F *Rev. Mod. Phys.*, 1963, 35: 23
49. Ovander, L N *Sov. Phys. Ups.*, 1965, 8: 337
50. Minck, R W, Terhune, R W and Wang, C C *Appl. Opt.*, 1966, 5: 1595
51. Akhmanov, S A and Khokhlov, R V *Sov. Phys. Usp*, 1968, 11: 394
52. Kielich, S *Opt. Electron.*, 1970, 2: 125
53. Kurtz, S K Nonlinear optical materials. In: *Laser Handbook*, vol 1, Arecchi, F T and Schulz-DuBois, E O (eds), North-Holland, Amsterdam, 1972, pp 923–974
54. Singh, S Nonlinear optical properties. In *Handbook of Laser Science and Technology*, Part 2, Pressley, R J (ed), Chem. Rubber Co. Press, 1971, pp 3–228
55. Shen, Y R *The Principles of Nonlinear Optics*, Wiley, New York, 1984
56. Chen, C and Liu, G *Annu. Rev. Mater. Sci.*, 1986, 16: 203
57. Gunter, P *Ferroelectrics*, 1980, 24: 35
58. Vidakovic, P V, Coquillay, M and Salin, F *J. Opt. Soc. Am. B*, 1987, 4: 998
59. Zyss, J *J. Non-Cryst. Solids*, 1982, 47: 211
60. Levine, B F, Bethea, C G, Thurmond, C D, Lynch, R T and Bernstein, J L *J. Appl. Phys.*, 1979, 50: 2523
61. Kato, K *IEEE J. Quantum Electron.*, 1980, QE-16: 1288
62. Ledoux, I, Josse, D, Vidakovic, P V and Zyss, J *Opt. Eng.*, 1986, 25: 202

63. Zyss, J, Nicoud, J F and Coquillay, M *J. Chem. Phys.*, 1984, 81: 4160

64. Oudar, J L and Hierle, R *J. Appl. Phys.*, 1977, 48: 2699

65. Zyss, J, Chemla, D S and Nicoud, J F *J. Chem. Phys.*, 1981, 74: 4800

66. Kerkoc, P, Zgonik, M, Sutter, K, Bosshard, C and Gunter, P *J. Opt. Soc. Am. B*, 1990, 7: 313

67. Bierlien, J D, Cheng, L K, Wang, Y and Tam, W *Appl. Phys. Lett.*, 1990, 56: 423 (b) Gotoh, T, Tsunekawa, T, Kondoh, T, Kukuda, S, Mataki, H, Iwamoto, M and Maeda, Y SPIE Proc., vol 1337, 1990, p. 272

68. Umegaki, S *Organic Nonlinear Optical Materials*, Bunshin Press, Tokyo, 1990 (Japanese)

69. Kerkoc, P, Zgonik, M, Sutter, K, Bosshard, C and Gunter, P *Appl. Phys. Lett.*, 1989, 54: 2062

70. Gunter, P, Bosshard, C, Sutter, K, Arend, H, Chapuis, G, Twieg, R J and Dobrowlske, D *Appl. Phys. Lett.*, 1987, 50: 486

71. Sutter, K, Bosshard, C, Ehrensperger, M, Gunter, P and Twieg, R J *IEEE J. Quantum Electron.*, 1988, QE-24: 2362

72. Nicoud, J F and Twieg, R J Design and synthesis of organic molecular compounds for efficient second-harmonic generation. In: *Nonlinear Optical Properties of Organic Molecules and Crystals*, vol 1, Chemla, D S and Zyss, J (eds), Academic, New York, 1987, pp 227–296

73. Zyss, J and Berthier, G *J. Chem. Phys.*, 1982, 77: 3635

74. Tieke, B *Adv. Mater.*, 1990, 2: 222

75. Stroeve, P and Franses, E *Thin Solid Films*, 1987, 152: 405

76. Peterson, I R *J. Phys. D: Appl. Phys.*, 1990, 23: 379

77. Watanabe, T, Yoshinaga, K, Fichou, D and Miyata, S *J. Chem. Soc. Chem. Commun.*, 1988, 250

78. Tomaru, S, Zembutsu, S, Kawachi, M and Kobayashi, M *J. Chem. Soc. Chem. Commun.*, 1984, 1207

79. Cox, S D, Gier, T E, Bierlein, J D and Stucky, G D *J. Am. Chem. Soc.*, 1989, 110: 2986

80. Sohn, J E, Singer, K D, Lalama, S J and Kuzyk, M G *Polym. Mater. Sci. Eng.*, 1986, 55: 532

81. Okamoto, N, Abe, T, Chen, D, Fujimura, H and Matsushima, R *Opt. Commun.*, 1990, 74: 421

82. Addadi, L, Berkovitch-Yellin, Z, van Mill, J, Shimon, L J W, Lahav, M and Leiserowitz, L *Angew. Chem. Int. Ed. Engl.*, 1985, 24: 466

83. Eaton, D F, Anderson, A G, Tam, W and Wang, Y *J. Am. Chem. Soc.*, 1987, 109: 1886

84. Yamamoto, H, Hosomi, T, Watanabe, T and Miyata, S *Nippon Kagaku Kaishi*, 1990, 7: 789

85. Tripathy, S, Cavicchi, E, Kumar, J and Kumar, R S *Chemtech*, 1989, 19: 620, 747

86. Flytzanis, C and Oudar, J L *Nonlinear Optics: Materials and Devices*, Springer, New York, 1986

87. Chemla, D S and Zyss, J *Nonlinear Optical Properties of Organic Molecules and Crystals*, vols 1 and 2, Academic, New York, 1987

88. Meredith, G R *Material Research Bulletin*, August 1988, pp 24–29

89. Nalwa, H S, Watanabe, T and Miyata, S Optical second harmonic generation in organic molecular and polymeric materials. In: *Photochemistry and Photophysics*, vol V, Rabek, J F and Scott G W (eds), CRC Press, Boca Raton, Florida, 1991

90. Williams, D J *Nonlinear Optical Properties of Organic and Polymeric Materials*, American Chemical Society, ACS Symp. Ser. No. 223, Washington D.C., 1983.

91. Heeger, A J, Orenstein, J and Ulrich, D R (eds) *Nonlinear Optical Properties of Polymers*, Materials Research Society Symposium, Proceedings No. 109, Pittsburgh, 1988

92. Kohayashi, T (ed) *Nonlinear Optics of Organics and Semiconductors*, Springer Proceedings in Physics, vol. 36, Springer-Verlag, Berlin, 1989

93. Hahn, R A and Bloor, D (eds), *Organic Materials for Nonlinear Optics*, Royal Society of Chemistry, London, 1990

94. Bredas, J L and Chance, R R (eds), *Conjugated Polymeric Materials: Opportunities in Electronics, Optoelectronics and Molecular Electronics*, Kluwer Academic Publishers, Dordrecht, 1990

95. Geoffroy, G L and Wrighton, M S *Organometallic Photochemistry*, Academic, New York, 1979

96. Frazier, C C, Harvey, M A, Cockerham, M P, Hand, H M, Chauchard, E A and Lee, C H *J. Phys. Chem.*, 1986, 90: 5703

97. Green, M L H, Marder, S R, Thompson, M E, Bandy, J A, Bloor, D, Kolinsky, P V and Jones, R J *Nature (London)*, 1987, 330: 360

98. Bandy, J A, Bunting, H E, Green, M L H, Marder, S R, Thompson, M E, Bloor, D, Kolinsky, P V and Jones, R J Ref. 92, p 219

99. Marder, S R, Perry, J W, Schaefer, W P, Tiemann, B G, Groves, P C and Perry, K J *SPIE Proc.*, vol. 1147, 1989, pp 108–115

100. Cheng, L T, Tam, W, Meredith, G R and Marder, S R *Mol. Cryst. Liq. Cryst.*, 1990, 189: 137

101. Tutt, L W, McCahon, S W and Klein, M B SPIE Proc., vol 1307, 1990, p. 315; Tutt, L W, McCahon, S W and Klein, M B, *Opt. Lett.*, 1990, 15: 700

102. Calabrese, J C and Tam W, *Chem. Phys. Lett.*, 1987, 133: 244

103. Briggs, T N, Jones, C J, McCleverty, J A, Neaves, B D and Colquhoum, H M *J. Chem. Soc. Dalton Trans.*, 1985, 1249

104. Al Obdaidi, N, Claque, D, Chaudhary, M, Jones, C J, McCleverty, J A, Pearson, J C and Salam, S S *J. Chem. Soc. Dalton Trans.*, 1987, 1733

105. Charsley, S M, Jones, C J, McCleverty, J A, Neaves, B D, Reynolds, S J and Denti, G *J. Chem. Soc. Dalton Trans.*, 1988, 293

106. Coe, B J, Jones, C J, McCleverty, J A, Bloor, D, Kolinsky, P V and Jones, R J *J. Chem. Soc. Chem. Commun.*, 1989, 1485

107. Tao, X T, Jiang, M H, Xu, D, Yuan, D R, Zhang, N and Shao, Z S *Proc. International Workshop on Crystal Growth of Organic Materials 7–9 December 1989, Tokyo, Japan*, Miyata, S (ed.), pp. 207–216

108. Zhang, N, Jiang, M H, Yuan, D R, Xu, D, Tao, X T and Shao, Z S *J. Cryst. Growth*, 1990, 102: 581

109. Tao, X, Zhang, N, Yuan, D, Xu, D, Yu, W and Jiang, M SPIE Proc., vol 1337, 1990, p 385

110. Tam, W, Eaton, D F, Calabrese, J C, Williams, I D, Wang, Y and Anderson, A G *Chem. Mater.*, 1989, 1: 128

111. Richardson, T, Roberts, G G, Polywka, M E C and Davies, S G *Thin Solid Films*, 1988, 156: 231

112. Tam, W and Calabrese, J C *Chem. Phys. Lett.*, 1988, 144: 79

113. Kanis, D R, Ratner, M A and Marks, T J *J. Am. Chem. Soc.*, 1990, 112: 8203

114. Chollet, P A, Kajzar, F and Moigne, J L SPIE Proc., 1991, vol 1237, 1990, p 87

115. Nalwa, H S, PhD Thesis, IIT, New Delhi, 1983

116. Marder, T B, Lesley, G, Yuan, Z, Stringer, G, Jobe, I R, Taylor, N J, Koch, L, Scott, K, Zelding, G, Williams, I D and Kurtz, S K Paper presented at 2nd International Symposium on Organic Materials for Non-linear Optics (OMNO '90), University of Oxford, UK, 4–6 September 1990

117. Thompson, M E, Myers, L K and Chiang, W E Paper presented at 2nd International Symposium on Organic Materials for Non-linear Optics (OMNO '90), University of Oxford, UK, 4–6 September 1990

118. Mignani, G, Kramer, A, Puccetti, G, Ledoux, I, Soula, G, Zyss, J and Meyrueix, R *Organometallics*, 1990, 9: 2640

119. Teng, C C and Garito, A F *Phys. Rev. Lett.*, 1989, 50: 350

120. Li, D, Ratner, M A, Marks, T J, Zhang, C H, Yang, ? and Wong, G K *J. Am. Chem. Soc.*, 1990, 112: 7389

121. Vizgert, R V, Davydov, B L, Kotovshchikov, S G and Starodubsteva, M P *Sov. J. Quantum Electron. (Engl. Transl.)* 1982, 12: 214

122. Andreichuk, A E, Durozhkin, L M, Krasilov, Y I, Maslyanitsyn, I A, Portnova, S M, Soboleva, L M, Khapaeva, L I, Chayanov, B A, Shigorin, V D and Shipulo, G P *Sov. Phys. Crystallogr. (Engl. Transl.)* 1983, 28: 547

123. Fumanova, N G, Razmanova, Z P, Soboleva, L V, Maslyanitsyn, I A, Siegert, H, Shigorin, V D and Shipulo, G P *Sov. Phys. Crystallogr. (Engl. Transl.)* 1984, 29: 285

124. Davydov, B L, Kotovshchikov, S K and Nefedov, V A *Sov. J. Quantum Electron. (Engl. Transl.)* 1977, 7: 129

125. Hermann, J P, Ricard, D and Ducuing, J *Appl. Phys. Lett.*, 1973, 23: 178

126. Rustagi, K C and Ducuing, J *Opt. Commun.*, 1974, 10: 258

127. Agrawal, G P, Cojan, C and Flytzasnis, C *Phys. Rev. B*, 1978, 17: 776

128. Flytzanis, C Ref. 91, p 167

129. Sixl, H *Adv. Polym. Sci.*, 1984, 63: 49

130. Kollmar, C and Sixl, H *J. Chem. Phys.*, 1987, 87: 5541

131. Koda, T, Ishikawa, K, Kanetake, 'T, Nishikawa, T, Tokura, Y, Koshihara, S, Takeda, K and Kudodera, K Paper presented at 3rd Asian Pacific Physics Conference, Hong Kong, June 1988

132. Tomaru, S, Kudodera, K, Kurihara, T and Zembutsu, S *Japanese J. Appl. Phys.*, 1987, 26: L1657

133. Hsu, C C, Kawabe, Y, Ho, Z Z, Peyghambarian, N, Polky, J N, Krug, W and Miao, E *J. Appl. Phys.*, 1990, 67: 7199

134. Wintner, E, Krausz, F and Leising, G *Synth. Metals*, 1989, 28: D155

135. Yang, L, Dorsinville, R, Wang, Q Z, Zou, W K, Ho, P P, Yang, N L, Alfano, R R, Zamboni, R, Danieli, R, Ruani, G and Taliani, C *J. Opt. Soc. Am. B*, 1989, 6: 753

136. Kaino, T, Kubodera, K, Tomaru, S, Kurihara, T, Saito, S, Tsutsui, T and Tokito, S *Electron. Lett.*, 1987, 23: 1095

137. Kaino, T, Kubodera, K, Saito, S and Tokito, S Microsymposium on Nonlinear Optical Organic Materials, The Society of Polymer Science, Japan, Tokyo, May 1989

138. Nalwa, H S *J. Phys. D: Appl. Phys.*, 1990, 23: 745; Nalwa, H S *Polymer*, 1991, 32: 745

139. Lindle, J R, Bartoli, F J, Hoffman, C A, Kim, O K, Lee, Y S, Shirk, J S and Kafafi, Z H *Appl. Phys. Lett.*, 1990, 56: 712

140. Jenekhe, S A, Chen, W C, Lo, S and Flom, S R *Appl. Phys. Lett.*, 1990, 57: 126

141. Takahashi, S, Morimoto, H, Murata, E, Kataoke, S, Sonogashira, K and Hagihara, N *J. Polym. Sci., Polym. Chem. Ed.*, 1982, 20: 562

142. Frazier, C C, Guha, S, Chen, W P, Cockerham, M P, Porter, P L, Chauchard, E A and Lee, C H *Polymer*, 1987, 28: 553

143. Frazier, C C, Chauchard, E A, Cockerham, M P and Porter, P L *Mater. Res. Soc. Symp. Proc.*, 1988, 109: 323

144. Guha, S, Frazier, C C, Parker, P L, Kang, K and Finberg, S E *Optics Lett.*, 1989, 14: 952

145. Moser, F H and Thomas, A H *The Phthalocyanines*, vols 1 and 2, CRC Press, Boca Raton, Florida, 1983

146. Berezin, B D *Coordination Compounds of Porphyrins and Phthalocyanines*, Nauk, Moscow, 1978

147. Meier, H *Organic Semiconductors*, Verlag-Chemie, Weinheim, 1974

148. Nalwa, H S *J. Electron. Mater.*, 1988, 17: 291

149. Nalwa, H S *Appl. Organomet. Chem.*, 1990, 4: 91 and references therein

150. Ho, Z Z, Ju, C Y and Hetherrington, W M, III, *J. Appl. Phys.*, 1987, 62: 716

151. Schaffer, A M and Gouterman, M *Theoret. Chim. Acta*, 1972, 25: 62

152. Klofta, T J, Rieke, P C, Linkous, C A, Buthner, W J, Nonthakumar, A, Mewborn, T D and Armstrong, N R *Electrochem. Soc.*, 1985, 132: 2134

153. Wada, T, Yamada, S, Matsuoka,. Y, Grossman, C H, Shigehara, K, Sasabe, H, Yamada, A and Garito, A F Ref. 93, pp 292–300

154. Shirk, J S, Lindle, J R, Bartoli, F J, Hoffman, C A, Kafafi, Z H and Snow, A W *Appl. Phys. Lett.*, 1989, 55: 1287

155. Casstevens, M K, Samoc, M, Pfleger, J and Prasad, P N *J. Chem. Phys.*, 1990, 92: 2019

156. Matsuda, H, Okada, S, Masaki, A, Nakanishi, H, Suda, Y, Shigehara, K and Yamada, A *SPIE Proc.*, vol. 1337, 1990, p. 105

157. Kajita, M, Ishikawa, K and Koda, T *Proceedings of 51st Meeting of Japanese Society of Applied Physics*, 1990, p 1011

158. Perry, J W, Khundkar, L R, Coulter, D R, Wei, T H, Van Stryland, E W and Hagan, D J in *Digest, Nonlinear Optics (NLO'90), Kauai, Hawai, 16–20 July 1990*, pp 61–62

159. Lindle, J R, Shirk, J S, Bartoli, F J, Kafafi, Z H, Snow, A W, Boyle, M E and Kim, O K *Proc. Symp. on New Materials for Nonlinear Optics*, American Chemical Society, Symp. Proc. vol XX, 1991, in press

160. Kaltbeitzel, A, Neher, D, Bubeck, C, Sauer, I, Wagner, G and Caseri, W *Electronic Properties of Conjugated Polymers*, vol III, Springer-Verlag, Berlin, 1989, p. 220; *Physics Abstracts*, 15 August 1989, No. 99434

161. Winter, C S, Oliver, S N and Rush, J D In: *Nonlinear Optical Effects in Organic Polymers*, Messier, J (ed), Kluwer, Dordrecht, 1989, pp 247–251, Opt. Commun., 1988, 69: 45.

162. Ghosal, S, Samoc, M, Prasad, P N and Tufariello J J *J. Phys. Chem.*, 1990, 94: 2847

163. Oliver, S N, Winter C S, Rush, J D, Underhill, A E and Hill, C SPIE Proc., vol 1337, 1990, p. 81

164. Miller, R D *Chem. Rev.*, 1989, 89: 1359

165. Miller, R D *Angew. Chem. Int. Ed. Engl. Adv. Mater.*, 1989, 28: 1733

166. Kajzar, F, Messier, J and Rosilio, C *J. Appl. Phys.*, 1986, 60: 3040

167. Yang, L, Wang, Q Z, Ho, P P, Dorsenville, R, Alfano, R R, Zou, W K and Yang, N L *Appl. Phys. Lett.*, 1988, 53: 1245

168. Baumert, J C, Bjorklund, G C, Jundt, D H, Jurich, M C, Looser, H, Miller, R D, Rabolt, J, Sooriyakumaran, R, Swalen, J D and Tweig, R J *Appl. Phys. Lett.*, 1988, 53: 1147

169. McGraw, D J, Siegman, A E, Wallraff, G M and Miller, R D *Appl. Phys. Lett.*, 1989, 54: 1713

170. Funatsu, E, Iwasa, Y, Koda, T, Kobayashi, H, Kodobera, K, Yamashita, M and Wada, Y *Proceedings of 51st Meeting of Japanese Society of Applied Physics*, 1990, p 1011

171. Wada, Y and Yamashita, M *Japanese J. Appl. Phys.*, 1990, 29: 2744

172. Tamir, T *Integrated Optics*, Springer-Verlag, Berlin, 1975

173. Boyd, G T *J. Opt. Soc. Am. B*, 1989, 6: 685

174. Gunter, P and Huignard, J P *Photorefractive Materials and Their Applications*, Springer-Verlag, New York, 1988

175. Mohlmann, G R, Horsthuis, W H G, Donach, A M, Copeland, M, Duchet, C, Fabre, P, Diemeer, M B J, Trommel, E S, Suyten, F M M, Van Tomme, E, Baquero, P and Van Daele, P *SPIE Proc.*, vol. 1337, 1990, p. 215

176. Mohlmann, G R *Synth. Metals*, 1990, 37: 207

177. Garito, A F and Wu, J W *SPIE Proc.*, vol 1147, 1989, pp 2–11

178. Gibbs, H M *Optical Bistability—Controlling Light by Light*, Academic, New York, 1985

179. Cahill, P A *Mater. Res. Soc. Proc.*, 1988, 109: 319

180. Schellenberg, F M, Byer, R L and Miller, R D *Optics Lett.*, 1990, 15: 242

181. Schellenberg, F M, Byer, R L, Miller, R D, and Kano, S *Mol. Cryst. Liq. Cryst.*, 1990, 183: 197

182. Zyss, J Ref. 94, pp 545–556

183. Pollagi, T P, Stoner, T C, Dallinger, R F, Gilbert, T M and Hopkins, M D *J. Am. Chem. Soc.*, 1991, 113: 703

184. Richardson, T, Roberts, G G, Polywka, M E C and Davies, S G *Thin Solid Films*, 1989, 179: 405

185. Sakaguchi, H, Nakamura, H, Nagamura, T, Ogawa, T and Matsuo, T *Chem. Lett.*, 1989: 1715

186. Sakaguchi, H, Nagamura, T and Matsuo, T *Japanese J. Appl. Phys.*, 1991, 30: L377

187. Matsuo, T, Nakamura, H, Shiromizu, T and Sakaguchi, H *Japanese Chemical Society 61st Meeting Proc.*, vol 61, 1991, p 323

188. Perry, J W, Stiegman, A E, Marder, S R and Coulter, D R In *Organic Materials for Nonlinear Optics*, Hahn, R A and Bloor, D (eds), Royal Society of Chemistry, London, Special Publication No. 69, 1989, p 189

189. Rao, D V G L N, Aranda, F J, Roach, J F and Remy, D E *Appl. Phys. Lett.*, 1991, 58: 1241

190. Maloney, C, Byrne, H, Dennis, W M, Blau, W and Kelly, J M *Chem. Phys.*, 1988, 121: 21

191. Devane, M M *Opt. Commun.*, 1984, 52: 136

192. Sakaguchi, T, Shimizu, Y, Miyama, S, Fukumi, T, Ota, K and Nagata, A *Japanese Chemical Society 61st Meeting Proc.*, vol 61, 1991, p 331

193. Shirk, J S, Lindle, J R, Bartoli, F J, Kafafi, Z H and Snow, A W *New Materials for Nonlinear Optics*, American Chemical Society Symp. Proc., vol XX, 1991, in press

194. Lindle, J R, Weisbecker, C S, Bartoli, F J, Shirk, J S, Yoon, T H, Kim, O K and Kafafi, Z H *Proc. Conference on Lasers and electro-optics (CLEO '91)*, abstract no QWC6, 1991

195. Sipp, B, Klein, G, Lavoine, J P, Penicaud, A and Batail, P *Chem. Phys.*, 1990, 144: 299